



MIDDLE EAST TECHNICAL UNIVERSITY
EARTHQUAKE ENGINEERING RESEARCH CENTER



**THE OCTOBER 30, 2020
İZMİR-SEFERİHİSAR OFFSHORE (SAMOS)
EARTHQUAKE ($M_w=6.6$)
RECONNAISSANCE OBSERVATIONS
AND FINDINGS**

REPORT NO: METU/EERC 2020-03

**NOVEMBER 2020
ANKARA**



MIDDLE EAST TECHNICAL UNIVERSITY
EARTHQUAKE ENGINEERING RESEARCH CENTER



**THE OCTOBER 30, 2020
İZMİR-SEFERİHİSAR OFFSHORE (SAMOS)
EARTHQUAKE ($M_w=6.6$)
RECONNAISSANCE OBSERVATIONS
AND FINDINGS**

REPORT NO: METU/EERC 2020-03

**NOVEMBER 2020
ANKARA**

Editor

Salim Azak

Acknowledgments

We would like to express our sincere thanks to the Office of the President of the Middle East Technical University, the Dean of the Faculty of Engineering, the Head of the Department of Civil Engineering, the Head of the Department of Geological Engineering and all the persons and organizations mentioned below, for their support and contributions before, during and after the emergence of this study.

METU Earthquake Engineering Research Center also would like to thank:

- The İzmir Metropolitan Municipality for providing great assistance during the field studies and researches,
- General Directorate of Infrastructure and Urban Transformation Services of the Ministry of Environment and Urbanization for their assistance in providing logistics, coordination, access and information regarding the observations and evaluations on building performance.
- Yüksel Project International Co. , TÜBİTAK, which supports under the project number 119Y419 and 5200101, Yıldız Technical University, Kocaeli University, İstanbul Metropolitan Municipality, Dokuz Eylül University, İzmir Metropolitan Municipality, Çeşme Municipality and Seferihisar Municipality, Dolfen Consultancy and Engineering, the authorities of Çeşme Marina, Sığacık Teos Marina and Port Alaçatı facilities, Dr. Zeynep Gülerce, faculty member of the Middle East Technical University Department of Civil Engineering, Mert Yaman, Ghazal Khodkar graduates of Middle East Technical University Department of Civil Engineering, Özgür Sarı Şahin, geomatic engineer from the Çeşme Municipality, Seçkin Demirel, geomatic engineer from the Seferihisar Municipality, map technicians Erhan Yükselen and Ömer Mede, for their contribution and support during the tsunami field observations,
- Construction Statistics Group of Turkish Statistical Institute for their contribution in the completion of the building stock characteristic of İzmir,
- Disaster and Emergency Management Presidency of Turkey that supports the tall building research project under grant UDAP- G-17-04, Mistral İzmir Management for authorizing the deployment of the structural health monitoring system, Ozan Çağlar İnaç for coordinating all these efforts and Süleyman Tunç for setting up the structural health monitoring system.

Authors

Chapter 2	
<i>Atilla Arda Özacar¹, Zeynep Gülerce¹, Eyüp Sopaç¹, Ayşegül Askan¹</i>	3
Chapter 3	
<i>Abdullah Altındal¹, Gizem Can¹, Shaghayegh Karimzadeh Naghshineh¹, Ayşegül Askan¹, Kemal Önder Çetin¹, Zeynep Gülerce¹, Atilla Arda Özacar¹</i>	9
Chapter 4	
<i>Ahmet Cevdet Yalçın¹, Gözde Güney Doğan¹, Yalçın Yüksel², Ergin Ulutaş³, Orhan Polat⁴, Işıksan Güler¹, Cihan Şahin², Utku Kanoğlu¹, Ahmet Tarih⁵, Evrens Rıza Yapar⁵, Evrim Yavuz⁵, M. Lütfi Süzen¹, Duygu Tüfekçi Enginar¹, Cem Bingöl¹, Sedat Gözlet¹, Hasan Gökhan Güler¹, Bora Yalçın¹, Atilla Arda Özacar¹</i>	15
Chapter 5	
<i>Kemal Önder Çetin¹, Zeynep Gülerce¹, Ayşegül Askan¹, Berna Unutmaz⁶, Mustafa Tolga Yılmaz¹, Atilla Arda Özacar¹, Shaghayegh Karimzadeh Naghshineh¹, Gizem Can¹, Makbule İlgaç¹, Elife Çakır¹, Berkan Söylemez¹, Moutasem Zerzour¹, Faik Cüceoğlu⁷, Alaa El Sayed¹, Ahmed Al-Suhaily¹, Soner Ocak¹, Eyüp Sopaç¹, Abdullah Altındal¹, DSİ Saha Araştırma Ekibi⁷</i>	23
Section 6.1	
<i>Bekir Özer Ay¹</i>	33
Section 6.2	
<i>Barış Binici¹, Erdem Canbay¹, Ahmet Yakut¹, Ozan Demirel¹, S. Selin Aktaş¹, Beyazıt Bestami Aydın¹, Batu Türksönmez¹</i>	36
Section 6.3	
<i>Ozan Cem Çelik¹</i>	42
Section 6.4	
<i>Alp Caner¹</i>	44

¹ Middle East Technical University

² Yıldız Technical University

³ Kocaeli University

⁴ Dokuz Eylül University

⁵ İstanbul Metropolitan Municipality

⁶ Hacettepe University

⁷ General Directorate of State Hydraulic Works

Contents

1	Introduction	1
2	Observations on İzmir-Seferihisar Offshore (Samos) Earthquake and Active Tectonism	3
3	Observations on the Recorded Strong Ground Motions.....	9
4	Post-Tsunami Field Observations.....	15
5	Geotechnical Reconnaissance Findings	23
5.1	Introduction	23
5.2	Directionality and Local Soil Site Effects	24
5.3	Seismic Soil Liquefaction	27
5.4	Building Foundations	28
5.5	Soil Slopes Instability and Rockfalls.....	30
5.6	Earthfill and Rockfill Dams	31
6	Observations and Evaluations on Structural Damage	33
6.1	Characteristics of the Building Stock in İzmir	33
6.2	Observations and Assessment of Building Performance.....	36
6.3	Tall Buildings.....	42
6.4	Bridges	44

Figures

Fig 2.1 a) Tectonic map showing epicenter (KOERI) of the mainshock with topography and bathymetry. Harvard CMT solution for the mainshock is given in the inset figure. b) Topographic map with Harvard CMT solutions of past events in the region. c) Map displaying aftershocks distribution (red filled circles; from AFAD), estimated rupture dimensions (yellow rectangle) and triggered seismicity at nearby faults (purple ellipse and white dotted line). Yellow star is the epicenter showing where earthquake started	4
Fig 2.2 Maps showing aftershock distribution in time (taken from AFAD)	5
Fig 2.3 Map of field observations points	6
Fig 2.4 Photos taken at the southern side of Dilek Peninsula showing uplifted terrace deposits	6
Fig 2.5 Active fault observations. Photos of south dipping normal faults near Kuşadası are given in a, b,c and e; Ephesus fault is in d and Gümüldür fault in f.	7
Fig 3.1 Locations of the strong ground motion stations (a) within 100 km epicentral distance, (b) selected for close investigation in this report	10
Fig 3.2 Acceleration time histories, Fourier amplitude spectra and response spectra of records at stations 0905, 3528, 3519, 3521, 3513 and 3514	11
Fig 3.3 Comparison of the observed ground motions with the predicted values from ASB2014 relationship	13
Fig 3.4 An estimated MMI map from the observed PGV values	13
Fig 4.1 Spatial and temporal distribution of 30 October tsunami a) source (generation) zone, b) propagation, c) amplification, and d) inundation computed by numerical modeling via NAMI DANCE	16
Fig 4.2 Post-tsunami field survey area where observations of tsunami waves were obtained from locals, debris or traces identified	18

Fig 4.3 Fisher boat on Alaçatı Azmak which was dragged 1162 m away from the shoreline (at 14:22 Local Time on 31 October 2020)	19
Fig 4.4 Tsunami traces on the garden fence of Teos Marina	19
Fig 4.5 Damage and tsunami traces in cafes and shops in Sığacık	20
Fig 4.6 Damaged fishery port piers, boats and small structures in Akarca due to tsunami	21
Fig 5.1 Geological map of the region, showing the routes followed, along with the locations of major reconnaissance findings.....	23
Fig 5.2 Bi-directional shaking paths at selected strong ground stations	24
Fig 5.3 (a) Digital elevation model of Gümüldür Region, (b) Geological cross-section passing through the bedrock outcropping next to the coast. (Demirtas (2019)).....	25
Fig 5.4 Typical borelogs from selected residential districts a) Gümüldür, b) Sığacık-Seferihisar, c) Mavişehir and d) Bayraklı	25
Fig 5.5 Elastic response spectra of select strong ground motion records	26
Fig 5.6 a) Potentially liquefiable alluvial basins and b) liquefaction hazard map released by USGS after the event	27
Fig 5.7 a) No surface manifestation (38.057442, 27.011747) b) Surface manifestations of seismic soil liquefaction in the form of sand boils (38.338447, 26.647494 and 38.310372, 26.679756).....	28
Fig 5.8 Illustrative foundation performances at selected sites: a) Germiyan (38.315925, 26.464742), b) Gümüldür (38.071206, 27.016639), c) Kuşadası (37.859711, 27.265708), d) Bayraklı (38.454033, 27.180125), e) Alsancak (38.439888, 27.145748) and f) Urla (38.321289, 26.770333).....	29
Fig 5.9 Liquefaction-induced bearing capacity failure in Adapazarı (on the left) after 1999 Kocaeli earthquake vs. tilted buildings due to partial failure of entrance floor columns and shear walls after İzmir-Seferihisar earthquake (on the right, coordinates:38.461689, 27.180669)	30

Fig 5.10 a) Fallen rock blocks (37.897341, 27.368394, b) A view from a highway cut with potential for slope instability (38.292119, 26.670731).....	30
Fig 5.11 Location of earthfill and rockfill dams, b) Ürkmez Dam Typical Cross-section and c) crest view of Ürkmez Dam.....	31
Fig 6.1 The number of buildings (left panel) and dwellings (right panel) in districts of İzmir	33
Fig 6.2 The percentages of reinforced concrete and masonry buildings in İzmir	34
Fig 6.3 The percentages of low-rise (1-3 story), mid-rise (4-8 story), and high-rise (+9 story) reinforced concrete buildings with respect to their time of construction	34
Fig 6.4 The percentages of buildings constructed from 1930 to 2019 in approx. ten years of the time interval.....	35
Fig 6.5 The variation of the average number of dwellings per building within years	35
Fig 6.6 Damage observed in Barış Building Complex.....	37
Fig 6.7 Damage observed in Cumhuriyet Building Complex.....	37
Fig 6.8 Damage observed in Adalet Building Complex	37
Fig 6.9 Egemen Building Complex, collapsed and undamaged looking buildings	38
Fig 6.10 Columns suffering excessive corrosion	39
Fig 6.11 Damage in the commercial center.....	39
Fig 6.12 Localized heavy damage.....	40
Fig 6.13 Instrumentation scheme	42
Fig 6.14 Floor accelerations and displacements.....	43
Fig 6.15 Inspected line	44
Fig 6.16 ASR based cracks (non-seismic) and general view	45
Fig 6.17 Typical before and after earthquake photo (December, 2019) & (November 2020).	45

Fig 6.18 Stopped construction of bridges 20 years ago without lateral girder stability (10 years ago and now)..... 46

Tables

Table 2.1 Earthquake and fault plane parameters of the mainshock compiled from different agencies.....	4
Table 3.1 Information on the selected stations.....	12
Table 5.1 List of inspected dams by DSI reconnaissance team	32

1 Introduction

On October 30, 2020 2.51 p.m. local time (UTC 11.51 a.m.), a moment magnitude (M_w) of 6.6 (according to AFAD, Disaster and Emergency Management Presidency; www.afad.gov.tr) or 6.9 (according to Kandilli Observatory and Earthquake Research Center, KOERI) earthquake occurred in Aegean Sea (<http://www.koeri.boun.edu.tr/sismo/2/30-ekim-2020-mw6-9-ege-denizi-izmir-depremi/>). Epicenter of the earthquake is approximately 10 km north of the Avlakia town in Samos Island and 23 km south of Doğanbey town in İzmir district. The İzmir-Seferihisar offshore (Samos) earthquake is noteworthy due to several different aspects, especially for the casualties (115 people) and significant structural damage observed in İzmir, Bayraklı that is located approximately 70 km away for the epicenter and the tsunami hitting the coastal area between Akarca and Sığacık towns of İzmir.

Members of the Middle East Technical University Earthquake Engineering Research Center (METU-EERC*) visited the damage-prone area immediately after the event. The reconnaissance study had covered a large area, starting from the Dilek Peninsula on the southwest corner up to İzmir Bornova on northeast. Separate teams have focused on different aspects of the earthquake, such as the indicators of fault deformation and earthquake activity, characteristics of recorded strong ground motions and possible site amplification effects, observed ground failures such as slope instability, lateral spreading and liquefaction, distribution and level of the structural damage, and observations on the tsunami and sea level change after the earthquake. This report summarizes the initial observations of the reconnaissance team, compiled within the first 10 days of the mainshock, and each subsection briefly discusses diverse aspects of the earthquake.

As the METU-EERC team, we are deeply sorry for the collateral damage and loss of lives in this earthquake and we would like to convey our condolences to the relatives of our citizens who lost their lives.

* <https://eerc.metu.edu.tr/en>

2 Observations on İzmir-Seferihisar Offshore (Samos) Earthquake and Active Tectonism

The İzmir- Seferihisar offshore (Samos) Earthquake has occurred on the north of Samos Island and west of Kuşadası Bay (yellow star in Fig 2.1). Earthquake focal mechanism solutions of the mainshock revealed almost pure extension along W-E oriented normal fault planes (inset in Fig 2.1a). The area is mainly dominated by the N-S directed extension accompanied by E-W oriented normal faults and lateral motions along NE-SW and NW-SE oriented strike-slip faults (Fig 2.1a). The moment tensor solutions of earthquakes with $M_w > 5$ since 1976 from Harvard CMT catalogue (<https://www.globalcmt.org/CMTsearch.html>) supports the coexistence of active extension and strike-slip deformation in the region (Fig 2.1b).

More than 2000 aftershocks were recorded within the first week of the earthquake as shown in Fig 2.1c. Among two nodal planes revealed by the computed mechanisms of the mainshock, the north-dipping plane is found to be better correlated with the tectonic model and the distribution of the aftershocks. Earthquake and fault plane parameters gathered from different agencies are provided in Table 2.1. Among available solutions, computed strike and rake are rather similar; while the dip amount varies significantly between 29° and 55° . Relocated aftershocks will help us to better constrain the dip amount of the fault plane in the near future.

The yellow rectangle shown in Fig 2.1c represents our preferred rupture dimensions. Epicenter location (KOERI, Table 2.1) with respect to the ruptured fault segment indicates unilateral rupture propagation towards west, which is in agreement with the Harvard CMT location (Table 2.1) representing where the major seismic moment release occurred during the mainshock. Aftershocks are more concentrated on the edges of the rupture plane and less concentrated within the rupture area where large moment release and thus slip is detected (finite fault model by S. Irmak; <https://twitter.com/TSirmak/status/1323029790790701056>). This preliminary finite fault model implies rather limited rupture dimensions that may indicate higher stress drop.

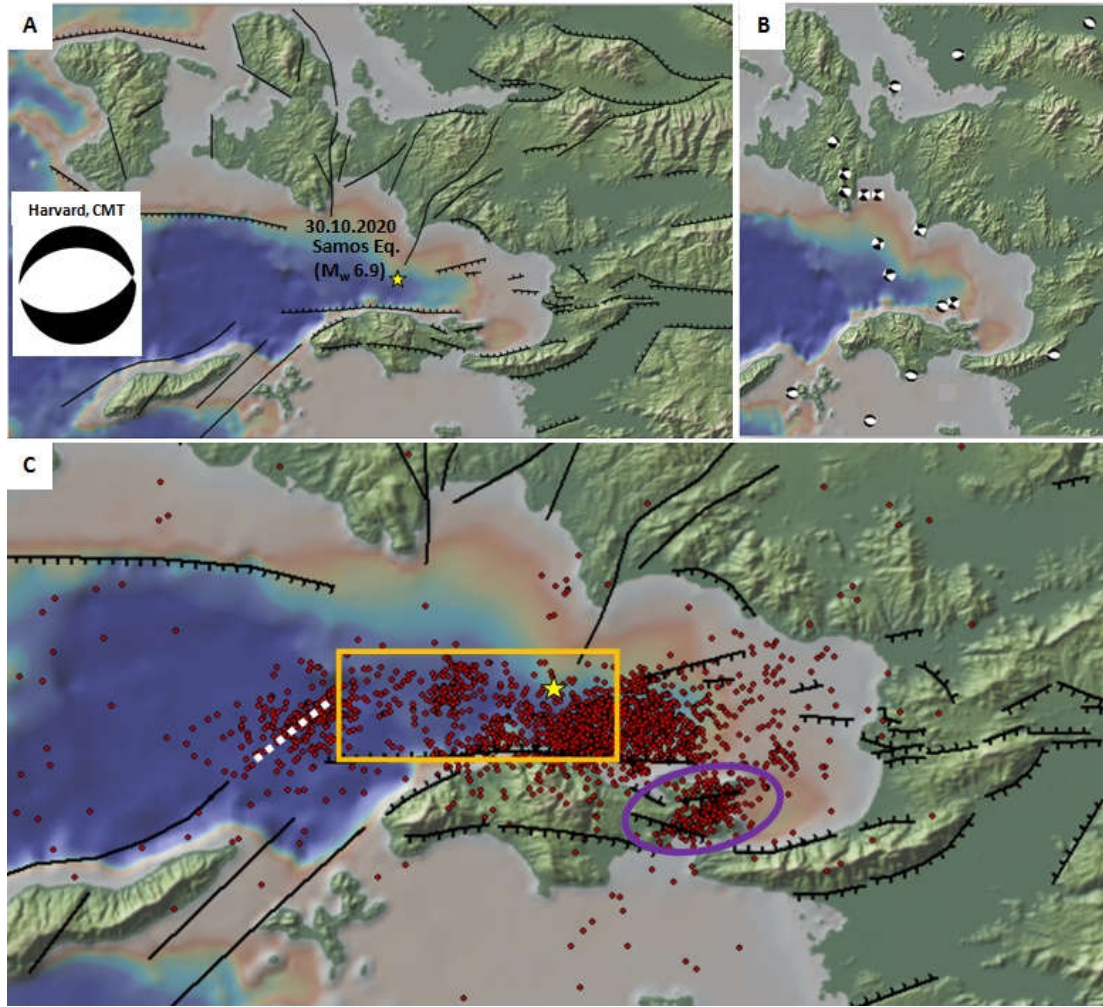


Fig 2.1 a) Tectonic map showing epicenter (KOERI) of the mainshock with topography and bathymetry. Harvard CMT solution for the mainshock is given in the inset figure. b) Topographic map with Harvard CMT solutions of past events in the region. c) Map displaying aftershocks distribution (red filled circles; from AFAD), estimated rupture dimensions (yellow rectangle) and triggered seismicity at nearby faults (purple ellipse and white dotted line). Yellow star is the epicenter showing where earthquake started

Table 2.1 Earthquake and fault plane parameters of the mainshock compiled from different agencies

Agency	M_w	Epicenter Coordinates	Depth (km)	Strike ($^{\circ}$)	Dip. ($^{\circ}$)	Rake ($^{\circ}$)
AFAD	6.6	37.888 $^{\circ}$ N - 26.777 $^{\circ}$ E	16	270	46	-91
KOERI*	6.9	37.902 $^{\circ}$ N - 26.794 $^{\circ}$ E	12	272	55	-93
USGS	7.0	37.918 $^{\circ}$ N - 26.790 $^{\circ}$ E	21	276	29	-88
CMT	7.0	37.760 $^{\circ}$ N - 26.680 $^{\circ}$ E	12	270	37	-86
GFZ	7.0	37.900 $^{\circ}$ N - 26.820 $^{\circ}$ E	15	272	48	-93

* Personal communication with Dr. Doğan Kalafat

It is important to note that the aftershocks also cluster outside the rupture area towards east and west, where the static stress change is expected to be high. Aftershocks may have activated a NE-SW directed strike-slip fault in west (shown with dashed white line in Fig 2.1c) and the fault segments located on the east of Samos Island (purple ellipse in Fig 2.1c). According to

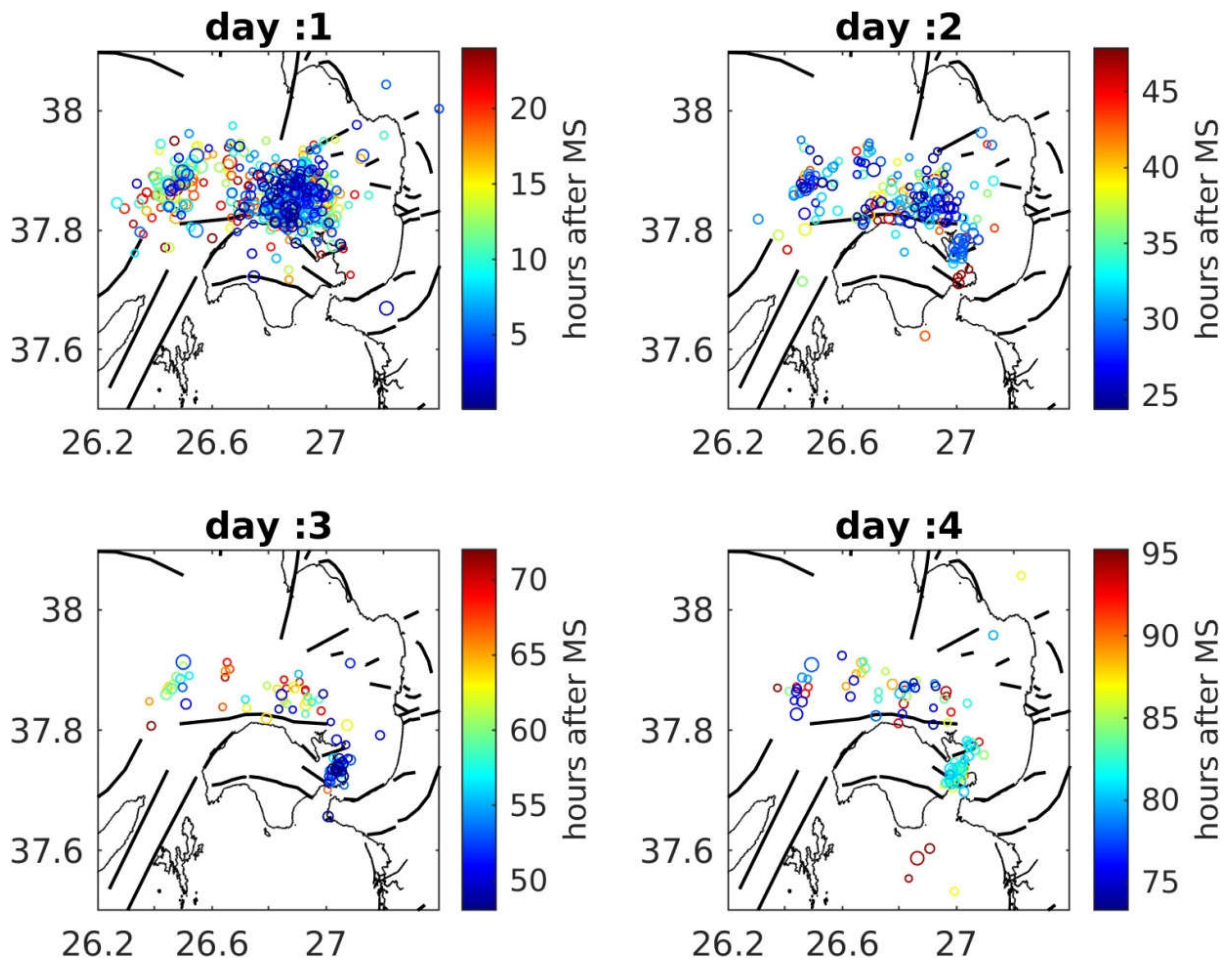


Fig 2.2 Maps showing aftershock distribution in time (taken from AFAD)

the time distribution of aftershocks recorded by AFAD in the first several days, there is a notable propagation in SW direction, especially after the first 24 hours of the mainshock (Fig 2.2). This is an indicator of a delayed seismic triggering on the small fault segments located on the eastern side of Samos Island and Dilek Peninsula (purple ellipse in Fig 2.1c and Fig 2.2).

During 2-day field excursion, a rather large area was investigated (Fig 2.3). On the southern side of the Dilek Peninsula, young uplifted terraces are detected in the coast supporting a rapid tectonic uplift associated to active normal faulting (Fig 2.4). In order to identify the permanent co-seismic ground deformations that may have occurred and to assess possible fault activations on the Turkish territory, NE-SW oriented strike-slip Tuzla and Seferihisar faults, E-W oriented normal faults near Kuşadası, Gümüldür, Selçuk, Söke and Dilek Peninsula were visited (Fig 2.3). Fig 2.5(a-e) and Fig 2.5f show the observed fault scarps of the active normal fault segments in Kuşadası Bay and Gümüldür coast, respectively. No indicators of co-seismic surface deformation were observed in any of these locations. Fault measurements collected on the normal faults revealed extension with occasional minor strike-slip component similar to the ruptured normal fault during the İzmir Seferihisar (Samos) earthquake. Some of these fault

scarps were quite close to residential buildings (e.g. Fig 2.5b, e, f); however, no structural damage was identified in the nearby structures.

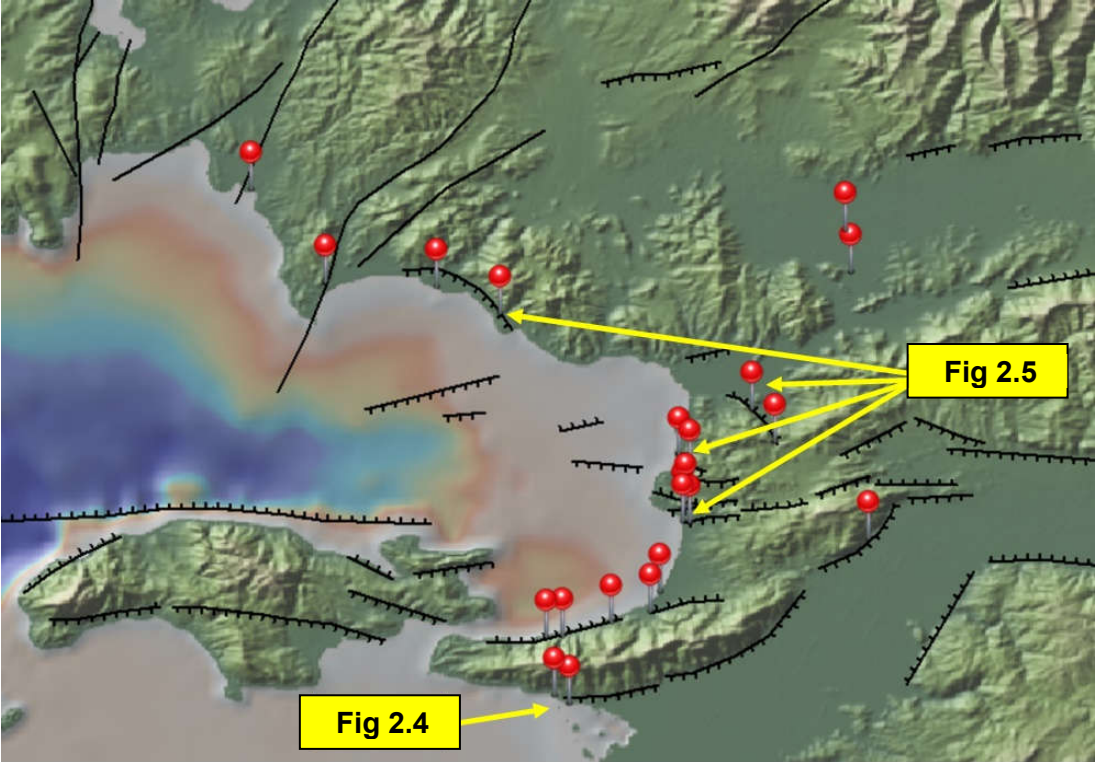


Fig 2.3 Map of field observations points



Fig 2.4 Photos taken at the southern side of Dilek Peninsula showing uplifted terrace deposits

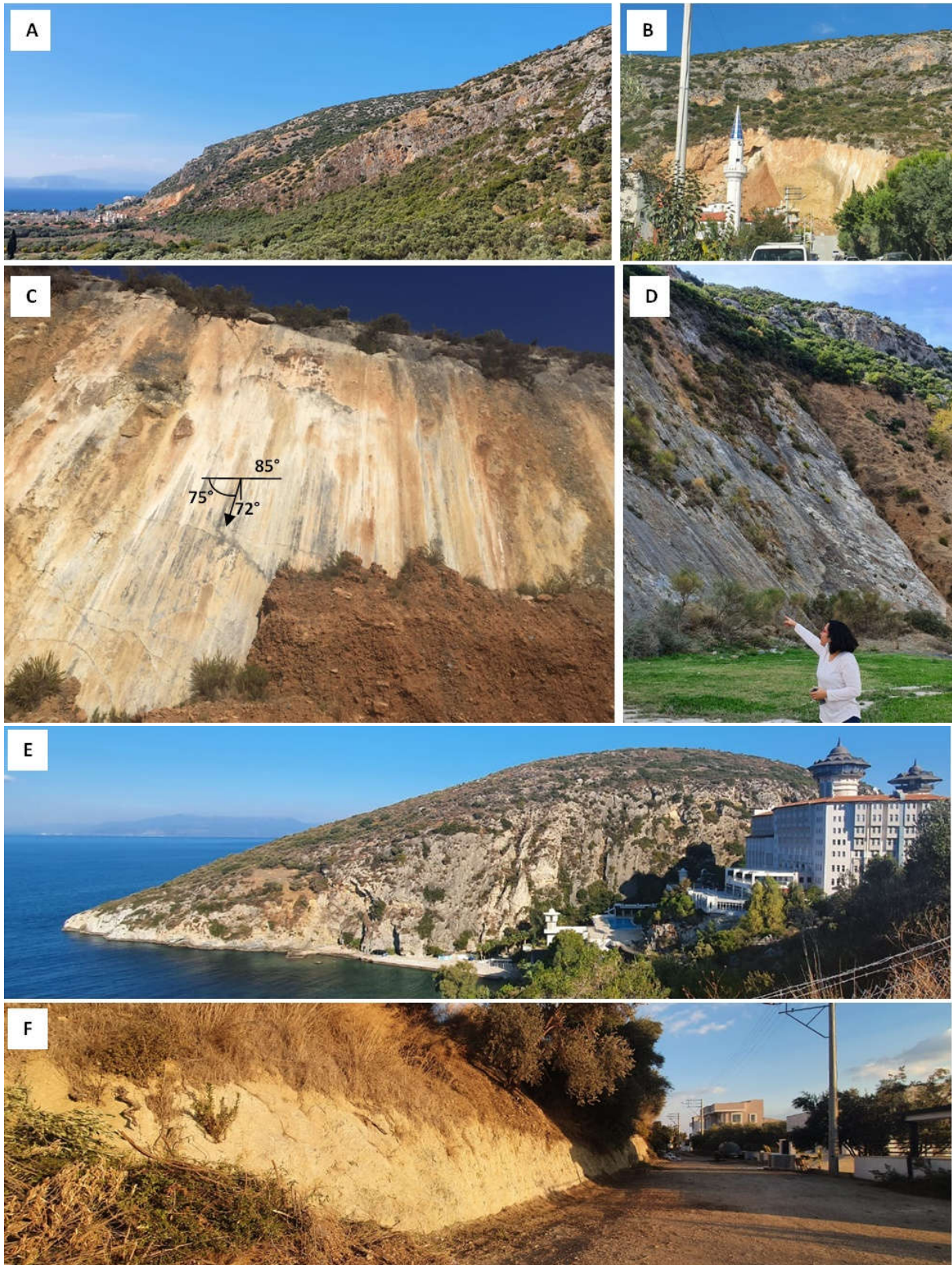


Fig 2.5 Active fault observations. Photos of south dipping normal faults near Kuşadası are given in a, b,c and e; Ephesus fault is in d and Gümüldür fault in f

3 Observations on the Recorded Strong Ground Motions

The mainshock of the 30 October İzmir- Seferihisar offshore (Samos) earthquake was recorded by 33 strong ground motion stations within 100 km distance from the epicenter (Fig 3.1). The data is recorded by strong ground motion network operated by AFAD. Both the raw and processed records are available at <https://tadas.afad.gov.tr>. The records show variability in terms of azimuth, source-to-site distances and site classes. In this report, time histories, Fourier amplitude spectra, and response spectra of the recorded accelerations at 6 selected stations are displayed in Fig 3.2. In the same figures, the response spectra are compared against the design spectra defined in the current and previous seismic codes in Turkey. Table 3.1 lists information on these records.

Among the selected stations, the one with the shortest distance from the epicenter is the station 0905 which is located on a stiff soil site ($V_{s30}=369$ m/s) in Kuşadası, Aydın and has the highest recorded peak ground acceleration (PGA) value of 0.18 g. Fourier amplitude spectra (FAS) and response spectra of the record indicate a short-period amplification within 0.2-0.3 seconds range, yet no significant structural damages are reported near this site. Station 3528, located in Çeşme Ilıca, is also on stiff soil ($V_{s30}=532$ m/s), has a PGA value of 0.15 g and shows short-period amplification. Two stations, stations 3519 and 3521 are located in Karşıyaka, İzmir on soft soil sites with NEHRP site class E with $V_{s30}=131$ m/s and 145 m/s, respectively. The records at these stations display long-period amplifications up to 1 s and 1.5 s, respectively.

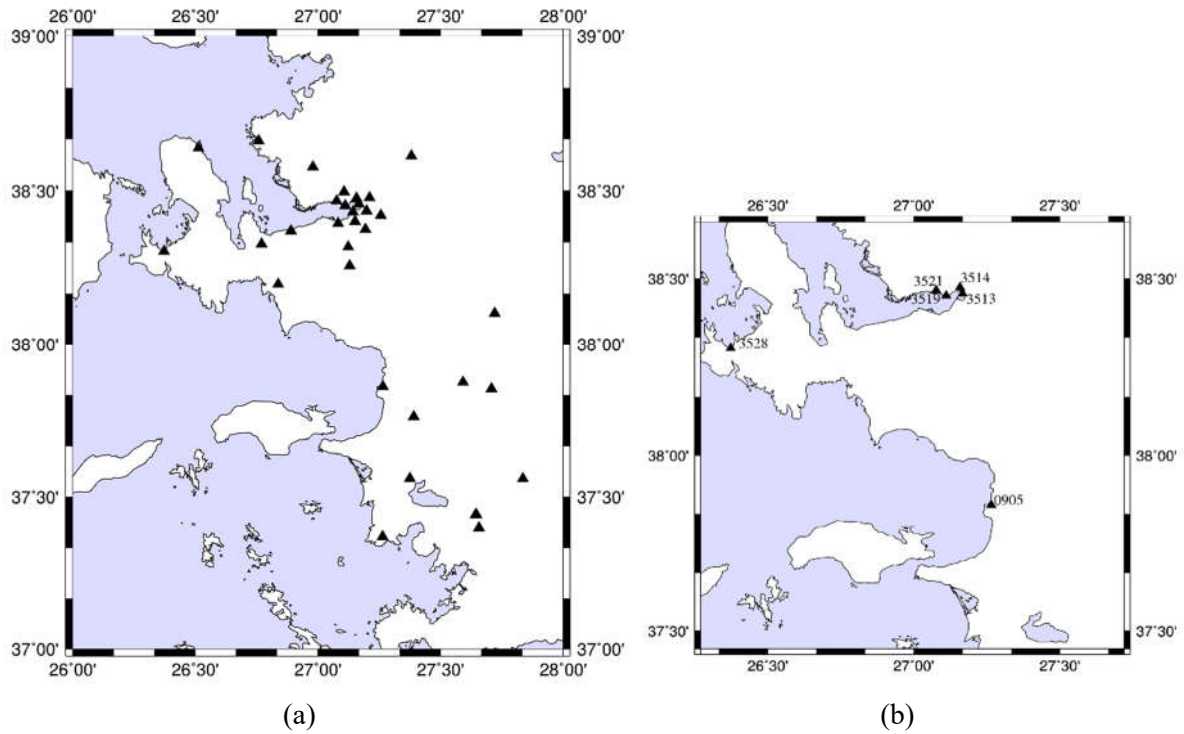


Fig 3.1 Locations of the strong ground motion stations (a) within 100 km epicentral distance, (b) selected for close investigation in this report

Stations 3513 and 3514 are both in Bayraklı region close to the structural failures and are located on soil ($V_{s30}=196$ m/s) and rock ($V_{s30}=836$ m/s) sites with site classes of D and B, respectively. At the station 3513, despite a low PGA level of 0.1 g, a clear long-period amplification is observed up to 1.5 sec. We note that at the rock station in Bayraklı region, station 3514, no similar amplifications are observed. Overall, longer significant durations are computed at softer sites.

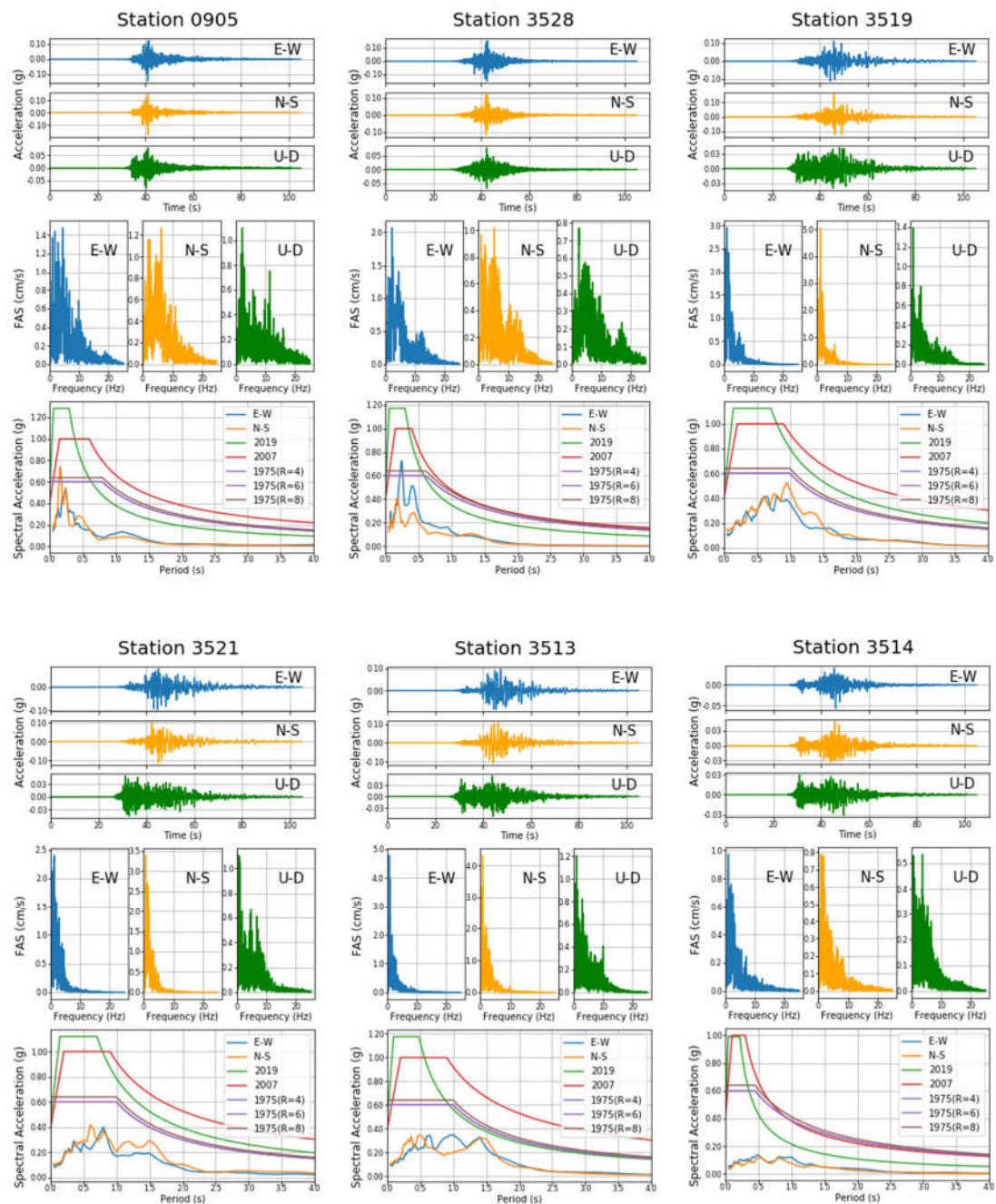


Fig 3.2 Acceleration time histories, Fourier amplitude spectra and response spectra of records at stations 0905, 3528, 3519, 3521, 3513 and 3514

At all stations, the observed spectra lie below the design spectra defined in the current seismic code of Turkey (TBEC, 2019). The same observation holds for the 2007 design spectra at all stations and for the 1975 design spectra except two stations. Yet, at stations 0905 and 3528, within short period range below 0.25 seconds, the spectral amplitudes are above the equivalent elastic spectra obtained from the inelastic design spectra of the 1975 seismic code with load reduction factors of R=4, 6 and 8. However, no structural collapses are reported nearby these stations.

Table 3.1 Information on the selected stations

Station Code	Repi (km)	Vs30 (m/s)	Direction	PGA (cm/s ²)	PGV (cm/s)	PGD (cm)	Significant Duration (s)	Arias Intensity (cm/s)	Housner Intensity (cm)
0905	42.95	369	E-W	144.017	8.93	2.257	16.61	20.37	35.6
			N-S	179.314	7.845	1.5	15.43	21.81	32.6
			U-D	79.839	4.556	1.347	17.88	8.38	20.1
3528	58.23	532	E-W	149.308	8.357	1.888	12.9	31.26	40.9
			N-S	117.571	7.571	2.258	14.77	14.33	32.7
			U-D	76.997	3.629	1.492	16.82	6.75	14.5
3519	69.23	131	E-W	109.975	14.479	3.237	23.17	35.95	76.8
			N-S	150.089	22.534	3.933	20.58	45.60	92.2
			U-D	34.173	4.333	1.049	31.06	6.00	22.9
3521	69.58	145	E-W	93.986	12.293	3.136	26.06	29.47	66.7
			N-S	110.844	16.174	4.08	22.61	35.19	87.4
			U-D	40.312	3.857	1.141	30.03	6.49	23.7
3513	72.00	196	E-W	94.667	14.422	3.152	20.16	35.30	84.8
			N-S	106.281	17.107	2.896	20.59	33.17	79.8
			U-D	44.186	4.483	0.795	30.84	6.42	23.3
3514	73.39	836	E-W	56.024	6.412	1.312	23.75	4.59	28.3
			N-S	39.421	4.225	1.444	25.9	3.52	22.4
			U-D	25.148	1.938	0.725	27.17	2.09	10.9

Next, a comparison of the recorded data within 100 km epicentral distance is made against the ground motion prediction equation (GMPE) by Akkar, Sandıkkaya and Bommer (Akkar vd., 2014). In Fig 3.3, comparisons between the predicted and observed data are made in terms of Vs30 values and epicentral distances, respectively. It is observed that some PGA values recorded at the soil sites and soft soil sites are above the corresponding median amplitudes predicted with the GMPE for Mw=6.6. This observation is consistent with the amplifications in the FAS and response spectra. Yet, use of a larger Mw value as suggested by KOERI or USGS could yield closer values to the observed data peaks.

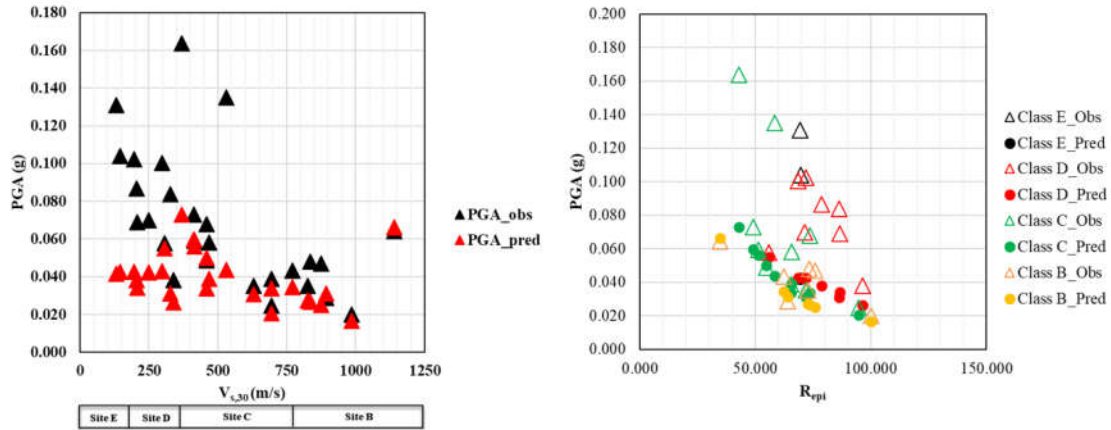


Fig 3.3 Comparison of the observed ground motions with the predicted values from ASB2014 relationship

Finally, an estimated intensity map in terms of Modified Mercalli Intensity (MMI) scale is prepared for the region. Intensity distribution maps are used to immediately estimate the areas of relative and maximum levels ground shaking. The empirical equations of Bilal and Askan (2014) are employed herein and MMI values are obtained from the observed PGV values. Fig 3.4 shows that majority of the region exhibits MMI values of V and VI while Bayraklı area has the maximum estimated MMI value of VII.

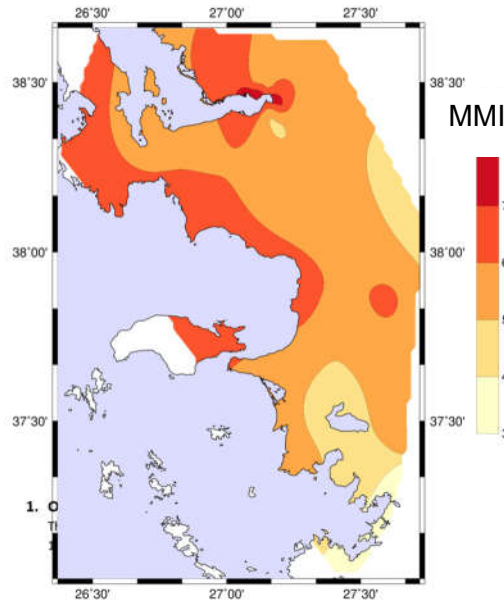


Fig 3.4 An estimated MMI map from the observed PGV values

4 Post-Tsunami Field Observations

A strong earthquake ($M_w=6.6$ AFAD, $M_w=6.9$ KOERI, $M_w=7.0$ USGS) of normal faulting striking about E-W occurred on October 30, 2020 (11.51 UTC) in between offshore Seferihisar (İzmir, Turkey) and Samos Island (Greece). The earthquake generated a tsunami that affected an area in the Aegean Coast of Turkey from Çeşme Alaçatı in the northwestern part to Gümüldür coast in the southeastern part.

Tsunamis leave different types of traces in the inundation zone after the event. These traces may disappear in a short time because of natural processes and human activities. Unfortunately, the tsunami was not recorded by any tide gauge located along the Turkish Coast of the Aegean Sea. Therefore, findings from the post-event survey have gained much more importance as the main documentation of sea level variations. Therefore, quick post tsunami field surveys are important to obtain undisturbed data of tsunami parameters. Measurements, eyewitness interviews and questionnaires are the main tools and methods to collect data and determine the tsunami parameters at the coastal and inundation zones.

Immediately after the event, a post-event field survey was performed on 31 October and 1 November 2020 by a team of seven people (A.C. Yalçiner, G.G. Doğan, E. Ulutaş and O. Polat, A. Tarih, E. R. Yapar and E. Yavuz) from METU, Kocaeli University, Dokuz Eylul University and İstanbul Metropolitan Municipality. This survey included more than 130 km of coast from Gümüldür to Alaçatı. On November 3rd, Arda Özacar and Zeynep Yılmaz Gülerce performed their investigation in Kuşadası-Davutlar Region. On 4-6 November 2020, for a more detailed survey, a second investigation has been done and A.C. Yalçiner, G.G. Doğan, Y. Yüksel, C. Şahin, U. Kanoğlu, I. Güler and Ö.S.Şahin participated to this investigation.

The Turkey coast survey area covers mainly three parts: i) Alaçatı and Zeytineli regions in the Northwestern, ii) Sığacık Bay and Akarca region in Seferihisar coast in the North, and iii) Tepecik and Gümüldür regions in the Northeastern with respect to the earthquake epicenter.

The team feels deep sorrow and express their condolences to the people for the loss of life and property in İzmir, Turkey and Greece.

This report is prepared to present the collected data obtained from the post tsunami field survey conveyed on 30 - 31 October and 4-6 November 2020 on the coast from Alaçatı to Gümüldür regions. The main objectives of this survey are to document the tsunami effects along the coast, obtain any available data on the observed coastal amplitudes and inundation extent, take pictures and audiovisual recording before they were cleaned, and interview the eyewitnesses and to understand and explain the event in detail.

According to the findings in this field survey and eyewitness reports, the most impacted areas were Sığacık Marina, Sığacık Bay and Akarca region located in a 30 km distance to the epicenter in the northern direction. In Sığacık locality, the maximum inundation distance reached 415 m whereas it was 285 m in Akarca, where 20 boats were sunk in a small fishery port. The inundation distance reached more than 2 km (2487 m) in Alaçatı Azmak Region. Fig 4.3 shows a fisher boat on Alaçatı Azmak which was dragged 1162 m away from the shoreline. In ancient Teos City, the tsunami inundation reached 552 m.

Tsunami generation zone which is calculated and visualized by modelling, propagation of the tsunami wave and wave run-up on coasts are shown in Fig 4.1 spatio-temporally. The modelling study has been done by NAMI DANCE Software, developed in METU and accepted worldwide. Ahmet Cevdet Yalçın, Gözde Güney Doğan, Bora Yalçın, Lütfi Süzen, Duygu Tüfekçi Enginar and Arda Özacar participated in modelling study.

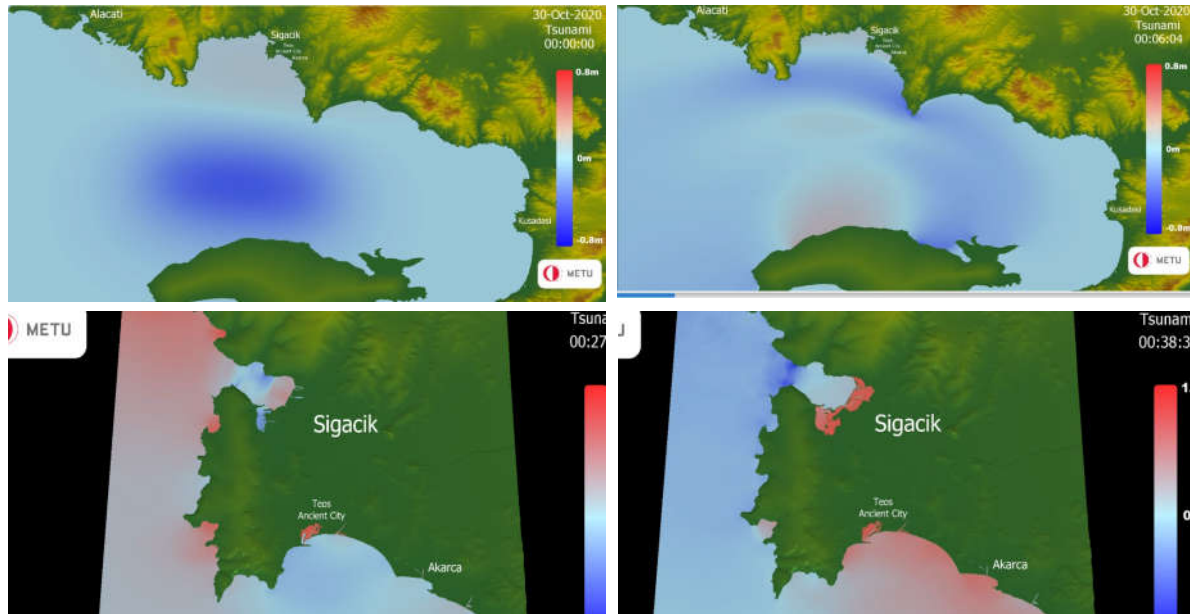


Fig 4.1 Spatial and temporal distribution of 30 October tsunami a) source (generation) zone, b) propagation, c) amplification, and d) inundation computed by numerical modeling via NAMI DANCE

Links for resulting animations of numerical modelling are presented below.

October 30th Tsunami Propagation – Large area (Sisam - İzmir) <https://bit.ly/3eHCAeI>

October 30th Tsunami Propagation – Small area (Sığacık) <https://bit.ly/36mejHc>

The maximum tsunami height, 2.31 m, measured in Sığacık Bay is obtained along the coast of Kaleiçi region. The maximum wave runup is measured as 3.82 m in Akarca Region at a location of 91 m inland. On the wall of a highly damaged house located just near the shore, which is on 0.89 m elevation, splash traces are found at 1.9 m height from the ground level. There was almost no significant inundation water motion after Gümüldür towards southeast. The tsunami impacts highly decreased after the cape of “V” shaped peninsula between Tepecik and Gümüldür. At Kuşadası Davutlar Sevgi Beach, tsunami traces are observed in the fishery port and the streambed entrance. Water level increased about 1 m at this region. On the northern part, the flow depth was measured as 1.9 m on the palm trees 50 m away from the coastline in Zeytineli Region.

To summarize, our findings show that in small bays with narrow entrances, the tsunami was much amplified and the impacts on these coasts were more severe. The region contains many streams (called Azmak in the local language) in the bays, which increases the potential of tsunami inundation and damage as also experienced in this event. Another important point is the remarkable increase in the awareness of the people who mostly moved away from the shore after noticing the sea withdrawal. However, unfortunately, a victim, who could not resist the strong current generated and died, was reported. After the 2017 Bodrum-Kos tsunami, the Aegean Sea with its high seismic mobility and this event once more reminded considerable tsunami potential in the eastern Mediterranean.

Fig 4.2 shows the survey area covered by the team, where the survey locations eyewitnesses were inquired, local authorities were contacted, measurements were taken, and observations on the tsunami waves and audiovisual recording were performed.

In the scope of field survey and investigations, questionnaires were conducted to evaluate the evacuation behavior of people effected by the earthquake and the tsunami. Questionnaires; which had been conducted before in Japan, Chile and Turkey after tsunami events; were carried out to understand the effect of tsunami on people’s evacuation behavior after strong earthquakes, how the people felt the earthquake and if the tsunami education affected their evacuation behavior. Thus, factors which can help to improve evacuation behavior are aimed to be identified. In this regard, questionnaires were conducted by Mehmet Sedat Gözlet, Cem Bingöl and Hasan Gökhan Güler on 5-6 November 2020 along the coast between Alaçatı - Gümüldür, on 14 November 2020 at Kuşadası-Davutlar, Kuşadası-Güzelçamlı and Didim, on 15 November 2020 at Kuşadası and on 16 November 2020 along the coast of Bodrum Peninsula. In addition to the questionnaires conducted, visual materials showing the behavior of people after the earthquake were gathered. The first results show that even if the earthquake is felt intensely, tsunami possibility was placed aside by people. Because of that, even if the people knew how to evacuate from the tsunami, they did not act accordingly. Furthermore, it is found that the earthquake victims tried to help the tsunami evacuation efforts where the sea

withdrawal was clearly observed and where the incoming tsunami wave was observed. The analysis results of questionnaires and visual materials are being conducted by Taro Arikawa, Ahmet Cevdet Yalçınır and Hasan Gökhan Güler. The results in detail will be presented as a report in the future.

Many coastal places were damaged by the tsunami in the field survey area causing material damage and financial loss which are given in Fig 4.3 -Fig 4.6.

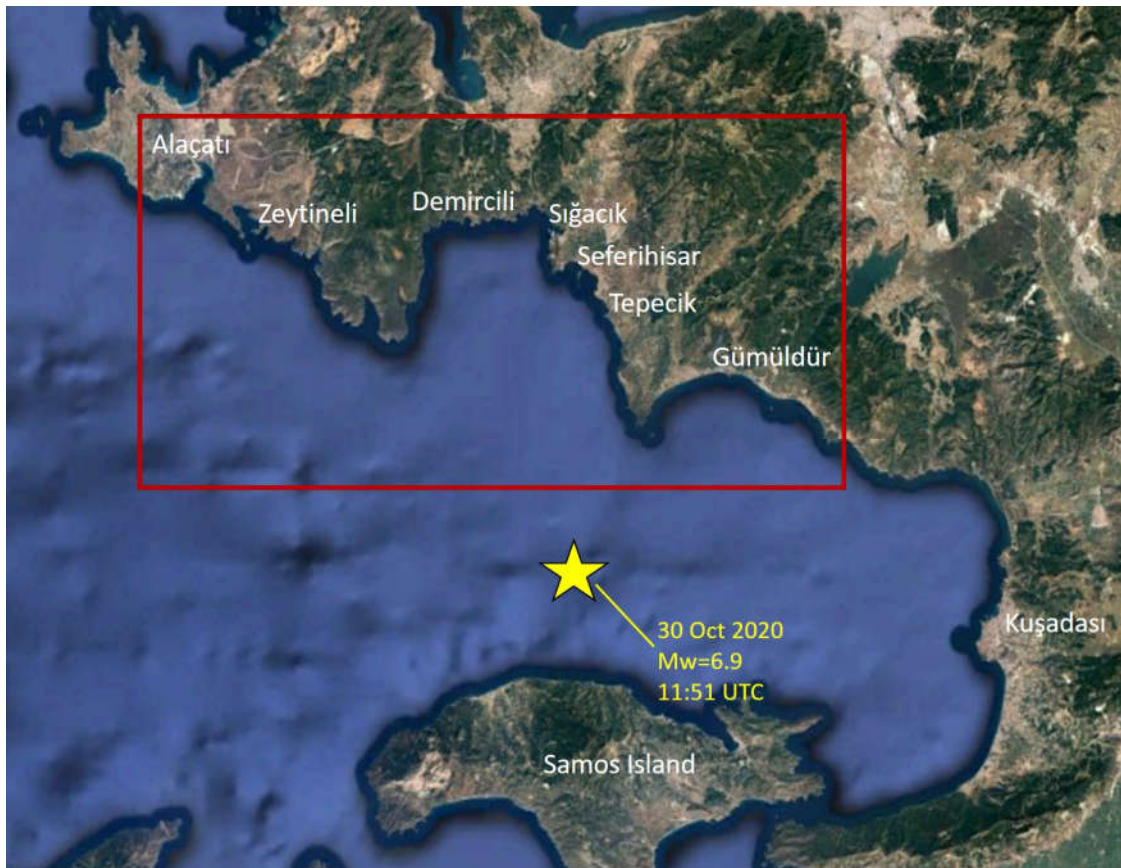


Fig 4.2 Post-tsunami field survey area where observations of tsunami waves were obtained from locals, debris or traces identified



Fig 4.3 Fisher boat on Alaçatı Azmak which was dragged 1162 m away from the shoreline (at 14:22 Local Time on 31 October 2020)

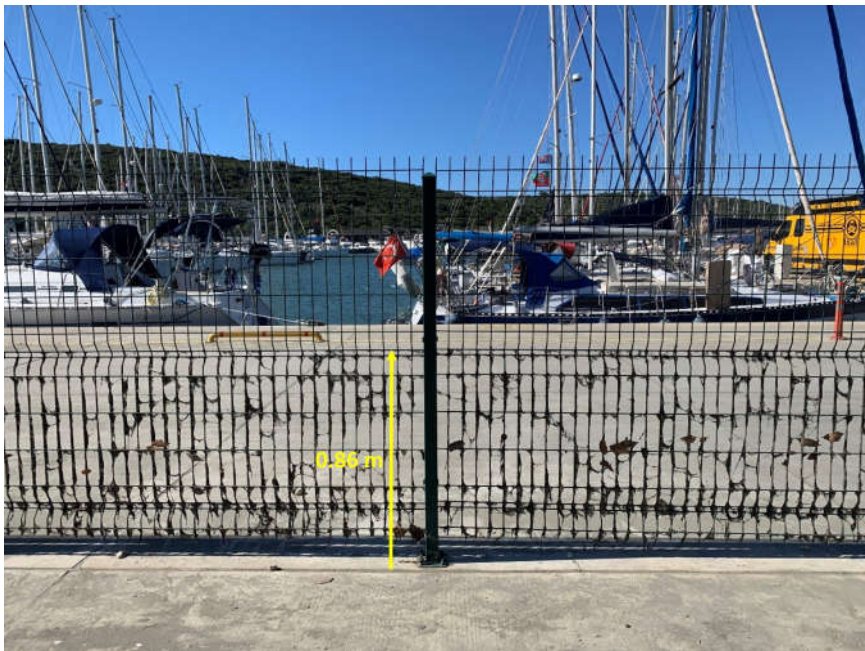


Fig 4.4 Tsunami traces on the garden fence of Teos Marina



Fig 4.5 Damage and tsunami traces in cafes and shops in Sığacık



Fig 4.6 Damaged fishery port piers, boats and small structures in Akarca due to tsunami

5 Geotechnical Reconnaissance Findings

5.1 Introduction

Immediately after the event, as of November 3, five geotechnical reconnaissance teams have been mobilized to the field to collect and document perishable geotechnical data. The route followed by these teams are shown in Fig 5.1, along with a summary of major geotechnical findings. More specifically, these efforts focus on the documentation and preliminary assessment of i) directionality and local soil site effects, ii) seismic soil liquefaction, iii) building foundation performance, iv) slope stability and rockfall sites, and v) seismic performance of earthfill and rockfill dams, which will be briefly discussed next. Please refer to “Geotechnical and Seismological Findings After Aegean Sea Samos Seferihisar-İzmir Earthquake” for a more complete and in-depth discussion of these.

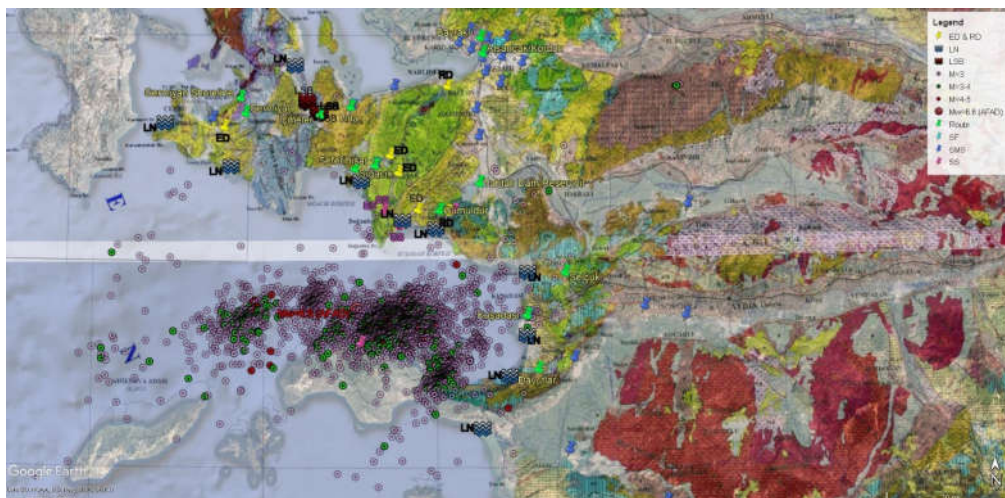


Fig 5.1 Geological map of the region, showing the routes followed, along with the locations of major reconnaissance findings

5.2 Directionality and Local Soil Site Effects

For a normal fault rupture, engineering structures are expected to be relatively more strongly shaken along fault normal direction on the hanging wall side of the rupture plane. Directionality effects are usually expected to be less pronounced with increasing distances from the zone of energy release. As shown in Fig 5.2, clear directionality effects were not observed at stations located neither relatively closely (e.g.: 3536) nor relatively far away (e.g.: 3513) locations.

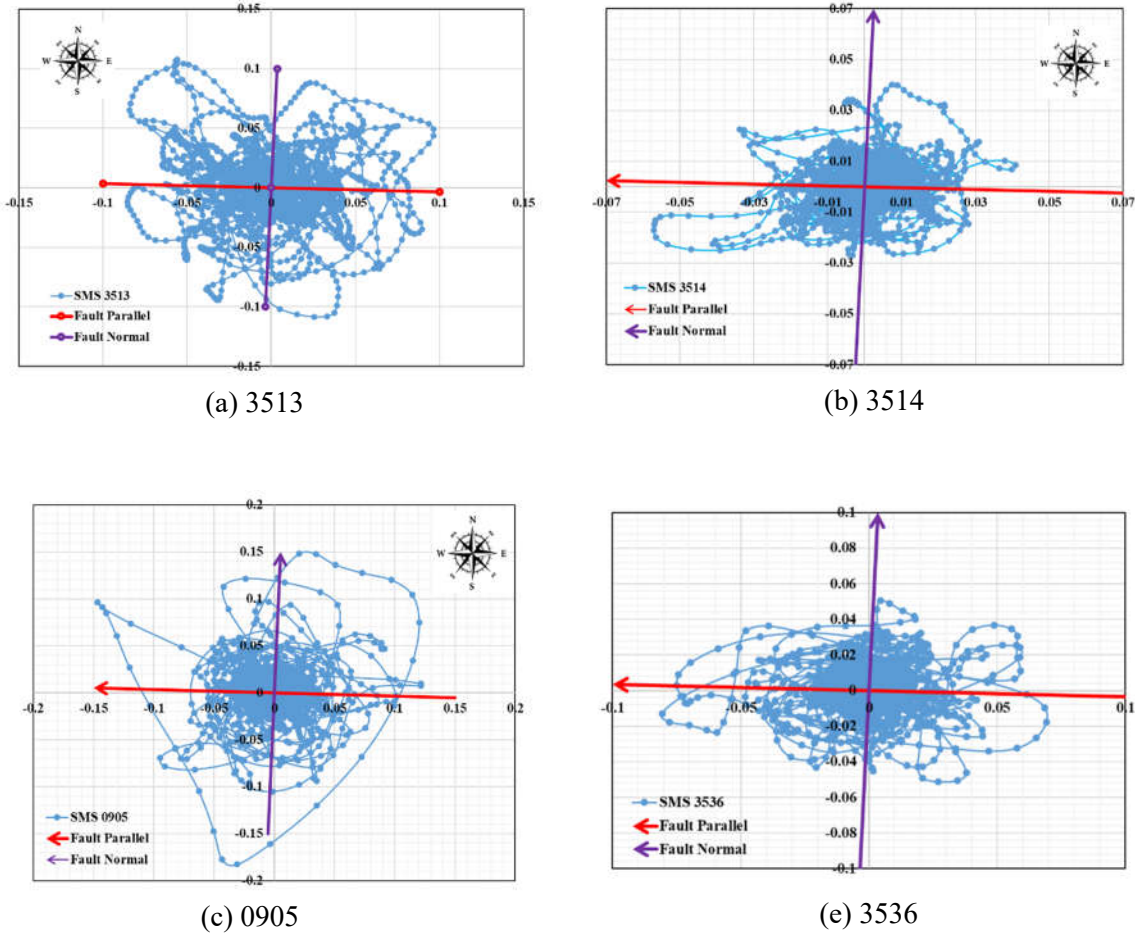
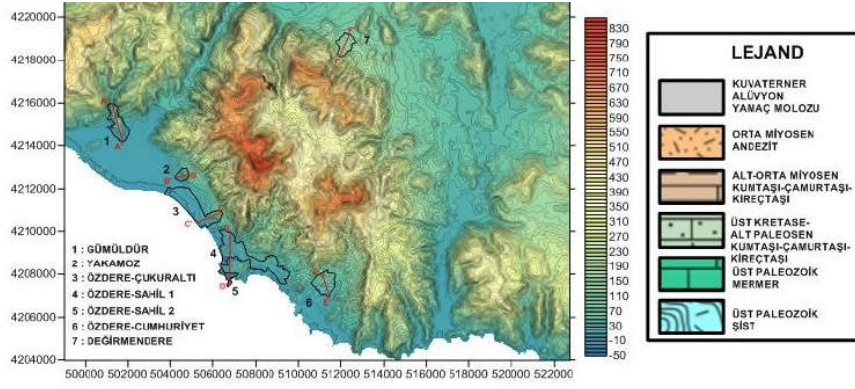
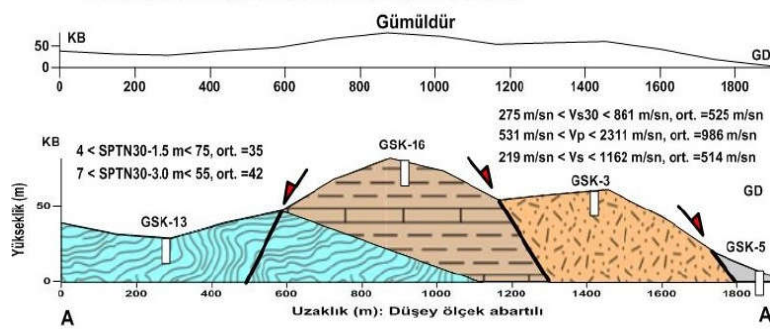


Fig 5.2 Bi-directional shaking paths at selected strong ground stations

Fig 5.3 presents surface geology map of Aegean Sea coasts in the vicinity of Gümüldür region. As clearly illustrated by this figure that the soil/rock site conditions of Aegean coastal region are mostly favorable (i.e.: weathered siltstone, sandstone, claystone, limestone, schist, stiff soil) with a few exceptions (e.g.: Sığacık). Despite relatively larger levels of shaking, relatively lower levels of structural damage are attributed to these favorable soil/rock site conditions along with other structural design, construction and detailing practices.



(a)



(b)

Fig 5.3 (a) Digital elevation model of Gümüldür Region, (b) Geological cross-section passing through the bedrock outcropping next to the coast. (Demirtas (2019))

For the purpose of assessing local soil site conditions, Fig 5.4 is prepared, which presents typical borelogs from selected residential districts. Deep alluvial soil layers underly residential structures at Bayraklı, Bornova and Mavişehir Districts.

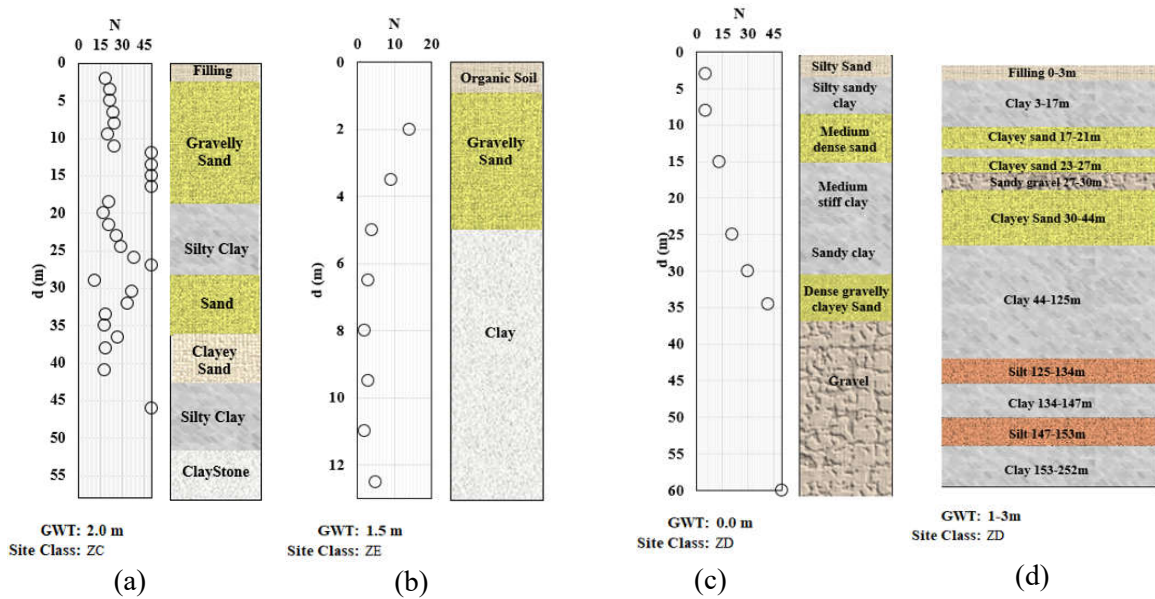


Fig 5.4 Typical borelogs from selected residential districts a) Gümüldür, b) Sığacık-Seferihisar, c) Mavişehir and d) Bayraklı

Surprisingly, at approximately 70 kilometers away from the source of energy release, deep soil sites at Bayraklı and Bornova districts were observed to be shaken by long period excitations approximately two to five times the intensity of a shallower stiff soil or rock site. This is illustrated by Fig 5.5. This, 2-5 times increased demand in higher periods due to local soil site effects resonated 7-12 story residential buildings, which is judged to contribute to the observed increased structural damage levels at deep alluvial soil sites (e.g.: Bayraklı and Bornova districts) accompanied by poor structural design, construction and detailing practices. It should be noted that the soil profile in Bayraklı consists of deep alluvial deposits, more specifically, of alternating thin gravel, silty sand, silty clay and clay layers, with SPT-N values less than 30 blows/30 cm in the upper 200 m. The groundwater table in Bayraklı is at 1-3 m depth. The depth to engineering bedrock layer is documented to vary in the range of 1100 m to 1200 m (Pamuk vd., 2017)

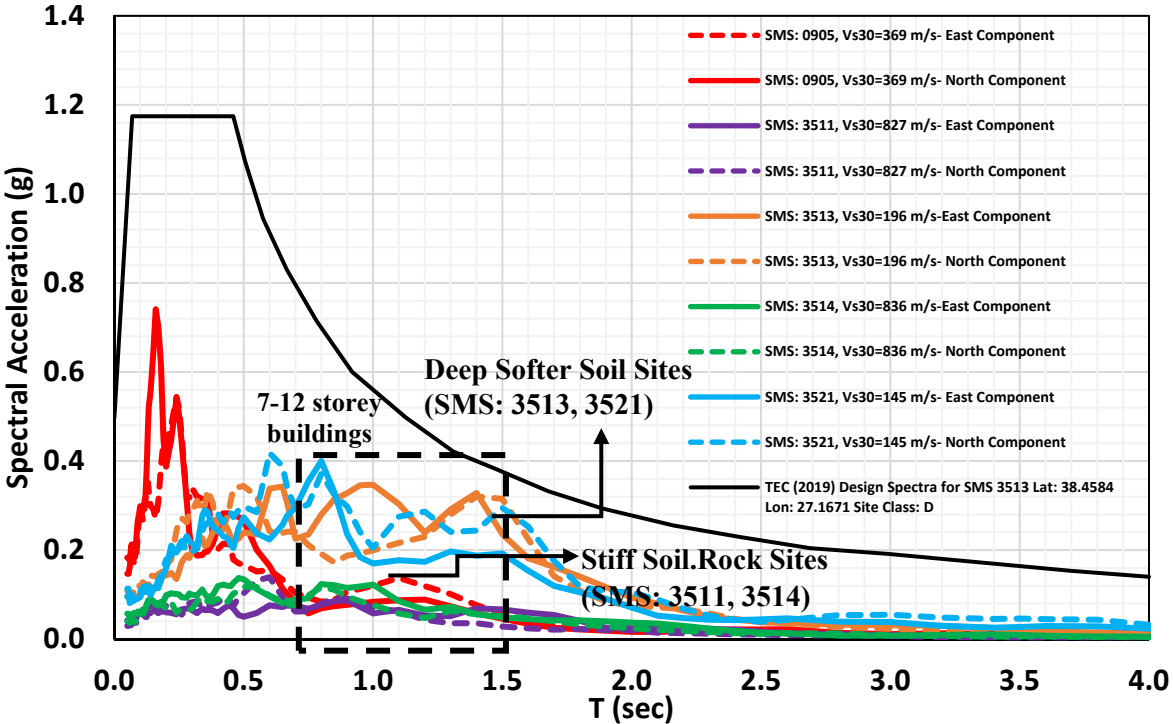


Fig 5.5 Elastic response spectra of select strong ground motion records

5.3 Seismic Soil Liquefaction

Potentially liquefiable alluvial basins are shown in Fig 5.6a. These regions are visited by the reconnaissance teams. Despite event specific liquefaction triggering predictions of the USGS as shown in Fig 5.6b, no surface manifestation of seismic soil liquefaction was seen at these basins located in the south of Seferihisar (Fig 5.7a). However, consistent with USGS predictions, at 45-50 kms away from the zone of energy release, along the shores of İçmeler and Gülbahçe districts, sand boils were observed (Fig 5.7b). These sites were in close proximity to Gülbahçe fault zone, and artesian pressures along with hot water springs are known to be present, which are also believed to contribute to the observed soil liquefaction triggering. The soil samples were retrieved from sand boils and soil ejecta, and they are to be tested at Civil Engineering Department Soil Mechanics laboratory at Middle East Technical University.

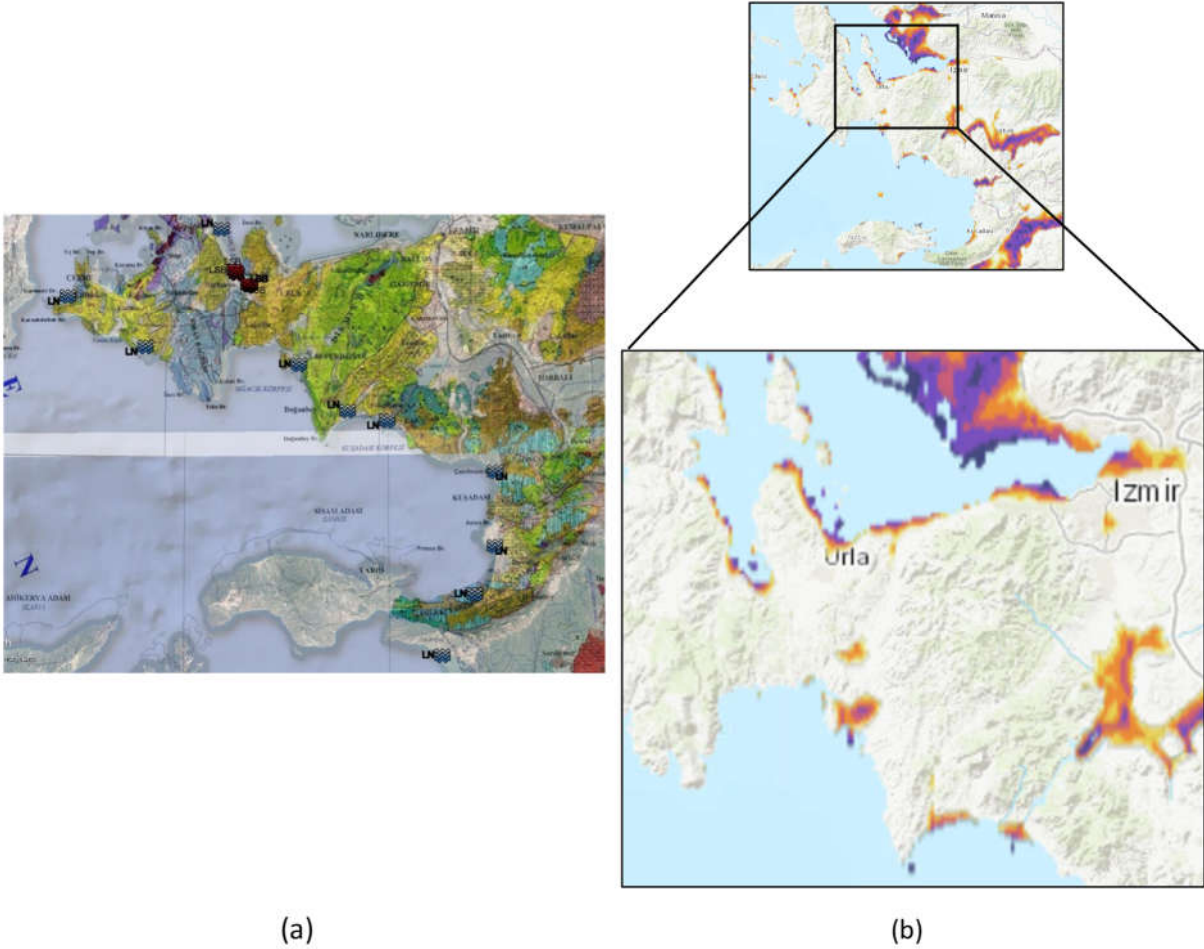


Fig 5.6 a) Potentially liquefiable alluvial basins and b) liquefaction hazard map released by USGS after the event



Fig 5.7 a) No surface manifestation (38.057442, 27.011747) b) Surface manifestations of seismic soil liquefaction in the form of sand boils (38.338447, 26.647494 and 38.310372, 26.679756)

5.4 Building Foundations

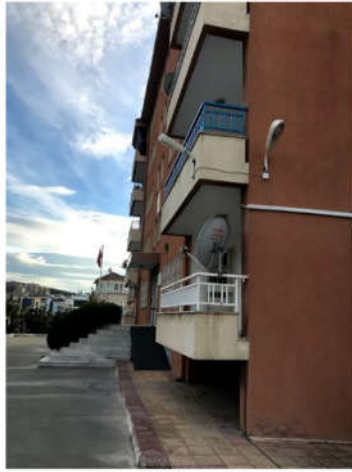
A number of structurally damaged residential buildings were also documented with special emphases on their foundation performances. Commonly, 1-2 story reinforced concrete beach houses were documented by the coastal region of Aegean Sea, starting from Çeşme in the north, to all the way down to Didim in the south. No apparent heavy structural damages were observed at these low-story light weight buildings. At downtowns of major districts, there exist 3 to 7 story reinforced concrete buildings founded on shallow, strip footings or individual footings with strapped beams. Again, no apparent evidence, suggesting excessive total or relative settlements, bearing capacity failures was mapped. A sample of illustrative pictures is presented in Fig 5.8.



(a)



(b)



(c)



(d)



(e)



(f)

Fig 5.8 Illustrative foundation performances at selected sites: a) Germiyan (38.315925, 26.464742), b) Gümüldür (38.071206, 27.016639), c) Kuşadası (37.859711, 27.265708), d) Bayraklı (38.454033, 27.180125), e) Alsancak (38.439888, 27.145748) and f) Urla (38.321289, 26.770333)

Despite unfavorable “soft” soil conditions, no apparent signs of surface manifestation of soil liquefaction, excessive settlement or bearing capacity-induced failures were mapped in Bayraklı and Bornova districts. In social media, the failure mechanism of some tilted buildings

due partial collapse of entrance floor columns and shear walls, were erroneously attributed to soil liquefaction and induced bearing capacity problems, which could not be verified in the field. A comparative illustration of “true” liquefaction-induced bearing capacity failures documented in Adapazarı after 1999 Kocaeli earthquake, is shown in Fig 5.9 along with tilted buildings from this event in Bayraklı district.



Fig 5.9 Liquefaction-induced bearing capacity failure in Adapazarı (on the left) after 1999 Kocaeli earthquake vs. tilted buildings due to partial failure of entrance floor columns and shear walls after İzmir-Seferihisar earthquake (on the right, coordinates:38.461689, 27.180669)

5.5 Soil Slopes Instability and Rockfalls

A limited number of rockfalls were observed by the benches of highways, one of which is illustrated in Fig 5.10a. Some potential landslide sites were also visited, but no signs of seismically induced movements were documented as also shown in Fig 5.10b.



Fig 5.10 a) Fallen rock blocks (37.897341, 27.368394, b) A view from a highway cut with potential for slope instability (38.292119, 26.670731)

5.6 Earthfill and Rockfill Dams

A reconnaissance engineering team was also assembled by İzmir Regional Directorate of State Hydraulic Works (DSİ) to document the performance of earthfill and rockfill dams, shaken by the event. On October 31, Ürkmez, Tahtalı, Kavakdere, Seferihisar, Alaçatı, Balçova dams in Küçük Menderes Basin were visited. Additionally, a METU team has also visited these dams. The dam body, crest, abutments, upstream and downstream slopes of the dam, as well as auxiliary structures (inlet, spillway, etc.) were investigated along with the evaluation of instrumental and visual inspection data. No apparent damage was reported at these dams. Location of the investigated dams and typical cross section of and Ürkmez dam along with the crest performance are shown in Fig 5.11.

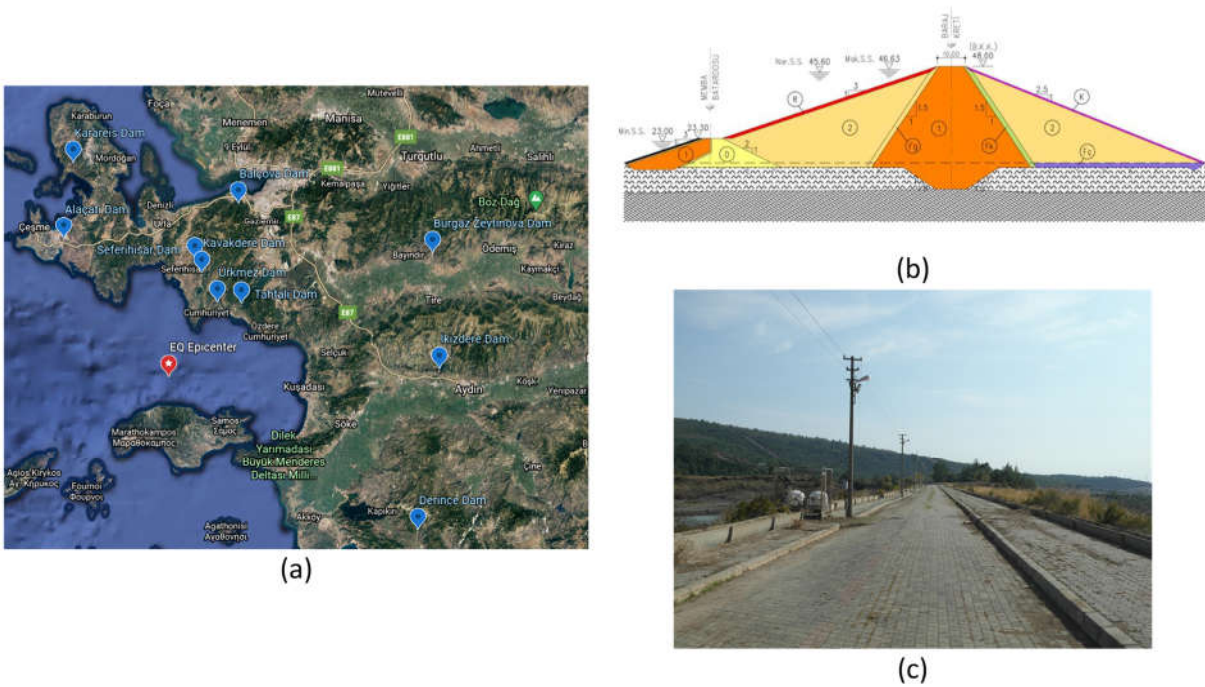


Fig 5.11 Location of earthfill and rockfill dams, b) Ürkmez Dam Typical Cross-section and c) crest view of Ürkmez Dam

Table 5.1 List of inspected dams by DSI reconnaissance team

	Ürkmez Dam	Tahtalı Dam	Kavakdere Dam	Seferihisar Dam	Alaçatı Dam	Balçova Dam
Location (District)	İzmir (Seferihisar)	İzmir (Menderes)	İzmir (Seferihisar)	İzmir (Seferihisar)	İzmir (Alaçatı)	İzmir (Balçova)
Purpose	Irrigation	Drinking Water	Irrigation	Irrigation	Drinking Water	Drinking Water
Completion (year)	1991	1996	2006	1994	1997	1980
Dam Type	Zoned Earthfill	Clay core Rockfill	Zoned Earthfill	Zoned Earthfill	Zoned Earthfill	Clay core Rockfill
Dam Volume (10³ m³)	981	-	2,100	1,485	275	1,011
Height from Foundation (m)	44.5	54.5	42	59	17.3	73.4
Active Storage (hm³)	7.57	306	13.6	28.18	16.11	7.94
Reservoir Area (km²)	0.61	25	0.96	1.79	42	0.69
Distance from EQ Epicenter (km)	26.7	32.2	33.9	37.5	54.6	58.5

6 Observations and Evaluations on Structural Damage

6.1 Characteristics of the Building Stock in İzmir

This section investigates İzmir's building stock characteristics, particularly reinforced concrete (RC) buildings, which constitute about 70% of the whole inventory in İzmir. The data compiled and presented below is taken from the 2000 Building Census (pre-2000 buildings) and Building Occupancy Permit Statistics (post-2000 buildings) disseminated by the Turkish Statistical Institute (TSI). TSI data does not include the buildings without permits in subdistricts and villages and squatter houses in large cities. According to the TSI data, about 670.000 buildings are containing 1.710.000 dwellings in İzmir (by the end of 2018). 88.5% of these buildings are used for residential or mostly residential purposes, whereas 11.5% are non-residential buildings (office buildings, hotels, industrial buildings, museums, etc.). Fig 6.1 shows the number of buildings (left panel) and dwellings (right panel) in İzmir at the district level.

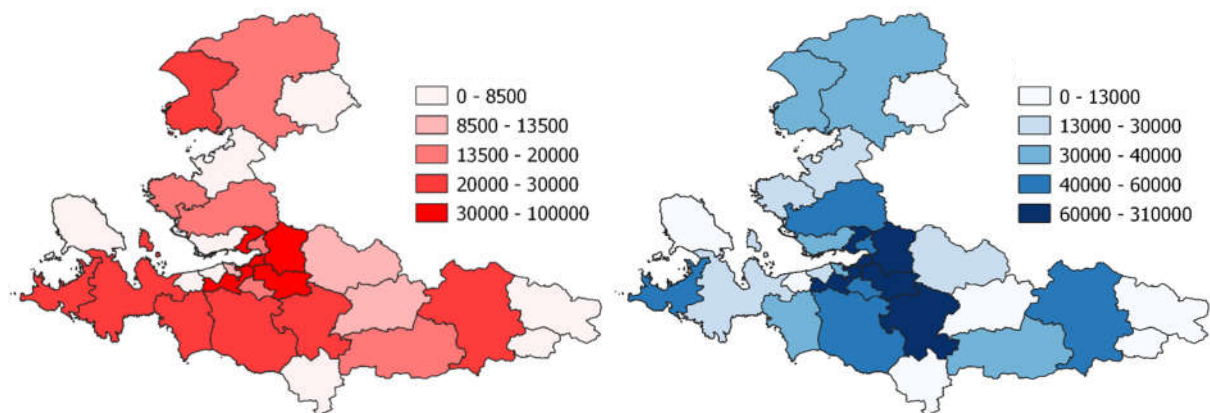


Fig 6.1 The number of buildings (left panel) and dwellings (right panel) in districts of İzmir

The building stock can be classified basically into three construction types: Reinforced concrete (frame, wall, and dual), masonry (load-bearing walls made of stone, clay brick, concrete block, etc.), and others (structural steel, wood frame, etc.). The statistics show that reinforced concrete and masonry buildings constitute 69% and 30% of the whole inventory, respectively, where the proportion of other buildings is not more than 1% (Fig 6.2).

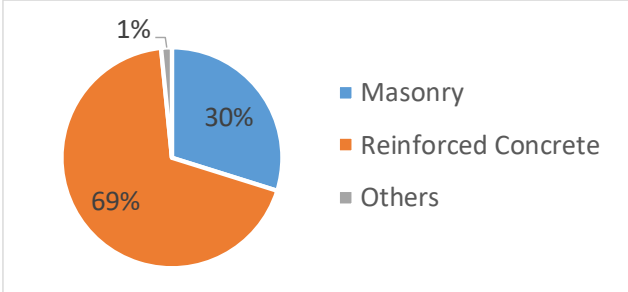


Fig 6.2 The percentages of reinforced concrete and masonry buildings in İzmir

Considering the resolution of TSI data in terms of the construction year and the structural design regulation that was in effect at the time of construction, reinforced concrete buildings can be classified into three as pre-1980 buildings, buildings constructed between 1980 and 2000, and post-2000 buildings. The number of story information can also be used as a primary classification parameter since this strongly influences the vulnerability of buildings, particularly that of reinforced concrete structures. The number of stories of reinforced concrete buildings in İzmir can be investigated in 3 groups as 1-3 story (low-rise), 4-8 story (mid-rise), and +9 story (high-rise) regarding their relative vulnerability observed in previous earthquakes in Turkey. Fig 6.3 displays the percentages of reinforced concrete buildings with respect to the construction year and the building height. The results show that the mid-rise (4-8 story) buildings constructed between 1980 and 2000, as one of the most vulnerable groups, constitutes about 11% (more than 50.000 buildings) of the reinforced concrete buildings in İzmir.

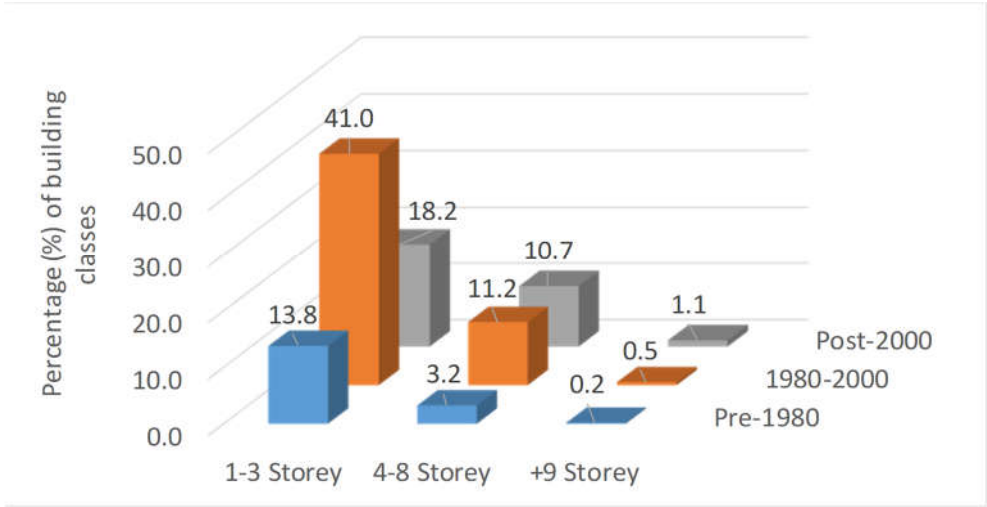


Fig 6.3 The percentages of low-rise (1-3 story), mid-rise (4-8 story), and high-rise (+9 story) reinforced concrete buildings with respect to their time of construction

Fig 6.4 compares the number of completed new buildings within approximately ten years of time intervals. The results clearly show the rapid increase in the number of new buildings constructed between 1980 and 2000. More than 40% of all the buildings in İzmir have been constructed within this 20-year period. The observations on damaged buildings after previous earthquakes in Turkey reveal that these buildings constitute one of the most vulnerable building classes in Turkey, and probably also in İzmir. The statistics presented in Fig 6.4 show that more than three-fourth of the building in İzmir (77.5%) have been constructed without conforming to modern design codes.

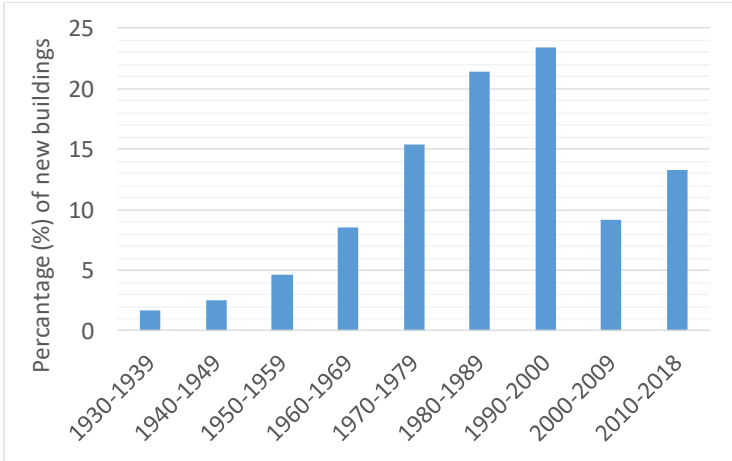


Fig 6.4 The percentages of buildings constructed from 1930 to 2019 in approx. ten years of the time interval

The building stock in İzmir can also be investigated in terms of the variation of the average number of dwellings per building within years. The results showed that the average dwelling number per building increases by 100% within the last forty years and by 50% within the last nine years, which indicates the frequent construction of high-rise buildings in İzmir (Fig 6.5). Regarding the average number of stories of buildings in districts of İzmir, Bayraklı has the highest value as 5.3, whereas Kınık has the lowest value as 1.3.

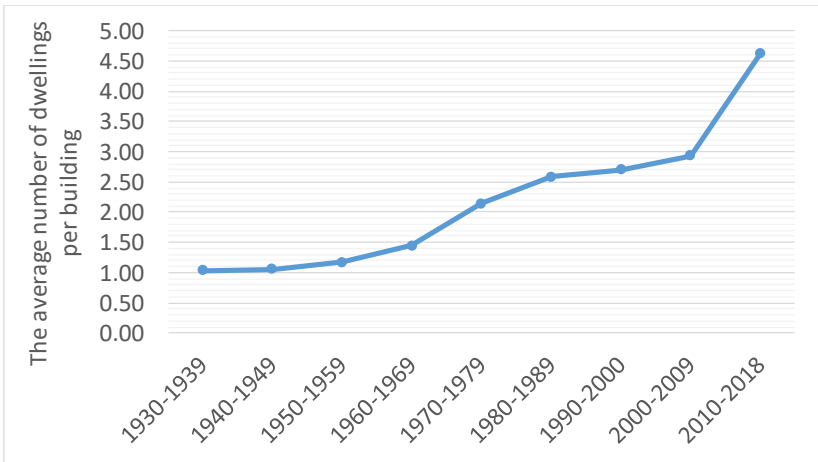


Fig 6.5 The variation of the average number of dwellings per building within years

6.2 Observations and Assessment of Building Performance

Some buildings located in Bayraklı district have suffered significant damage during İzmir-Seferihisar offshore (Samos) earthquake despite their locations being more than 60 km from the epicenter. Damage assessment studies conducted by the Ministry of Environment and Urbanization revealed that 13 buildings collapsed and nearly 110 buildings suffered heavy damage. Besides, in many buildings, nonstructural damage on infill walls and infill-frame interfaces was observed. Our field damage survey, which focused on Bayraklı district where the damage has concentrated, investigated, especially the buildings suffering total collapse and those around them with relatively less damage.

Examination of the ground motion records presented earlier in this report shows that the spectral acceleration measured at the soft soils in Bayraklı is around 0.35g in the period range of 0.8-1.4 seconds. According to Turkey's current seismic hazard map, these values are above the spectral accelerations corresponding to a ground motion level of service earthquake (72-year return period). Still, they are around 30-40 percent of the design level earthquake ground motion (475-year return period). For this reason, it appears that the earthquake led to heavy damage for 7-10 story buildings designed between 1990-1994 with major inadequacies. These types of damages were observed in Barış Building Complex (4 buildings with 9 stories, Fig 6.6), Cumhuriyet Building Complex (3 buildings with 8 stories, Fig 6.7), and Adalet Building Complex (2 buildings with 9 stories, Fig 6.8). Although the buildings within each of these complexes have identical plan properties (area, plan drawings), different damage levels were observed. Two buildings in Barış Apartment Complex had experienced total collapse, one building suffered heavy damage, and the fourth building survived the earthquake with minimal structural damage and significant infill wall damage. The two main reasons for the building to survive the earthquake are; 1) unlike three other buildings, this building had a significant amount of infill walls in the ground floor allocated for management office and superintendent flat, 2) this block was constructed by a different contractor with most probably a better construction quality. Our assessments revealed that the presence of infill walls and the difference in the quality of construction had increased the base shear capacity of the building by approximately 20-30 percent. The past observation that infill walls help the buildings survive small to medium size earthquakes by contributing to their lateral load carrying capacity was confirmed. A similar observation can be made in Cumhuriyet complex, where the level of damage in one building is limited but in the other two buildings are more significant.



Fig 6.6 Damage observed in Barış Building Complex



Fig 6.7 Damage observed in Cumhuriyet Building Complex



Fig 6.8 Damage observed in Adalet Building Complex

Another case where our observations focused was the Egemen Building Complex with two similar buildings. Although the first two floors of one of the buildings collapsed, almost no damage was observed from the street survey. The building's assessment from inside revealed heavy shear damage and significant corrosion in columns (Fig 6.9). This observation clearly shows that damage assessment based on building examination without entering inside may lead to quite misleading results.



Fig 6.9 Egemen Building Complex, collapsed and undamaged looking buildings

Our investigations showed that corrosion in reinforcement is a widespread problem in İzmir (Fig 6.10). Excessive corrosion was especially observed at the lower end of columns located in the basement of ground floors. The loss in the cross-sectional area of reinforcement due to corrosion was significant in some instances reaching values from 25 to 65 percent.

The widespread nonstructural damage observed in a recently constructed commercial center points out some design mistakes (Fig 6.11). This 10-story commercial center has a shear wall core and a large opening in the center of the slab. All offices are located around the opening. Although no damage was observed in the shear wall, heavy shear cracks were observed in the infill walls. It is surprising to see such heavy level of infill wall damage in a recently constructed building under an earthquake ground motion well below the design earthquake level. We believe that due to lack of diaphragm action, the core wall was unable to restrain the interstory drift. It appears that improper modelling and inadequate design led to excessive drift of office areas, and the infill walls around offices suffered heavy damage. This observation emphasizes the importance of slab openings (slab discontinuity) and ways for developing proper load transfer mechanisms to the shear walls.



Fig 6.10 Columns suffering excessive corrosion



Fig 6.11 Damage in the commercial center

The damage in other assessed buildings (Sezen complex, Özkaymak complex, Yazıcıoğlu complex, Canbazoğlu complex, Dilara apartment) generally was moderate to severe, but due to shear cracks observed in some columns (less than 1 mm) and, permanent vertical and lateral deformations (nearly 2 mm cantilever tip settlement), these buildings could not be re-occupied (Fig 6.12). The damage observed in overhangs, cantilever connections, and ground floor columns did not lead to collapse but prevented re-occupation.

Another major drawback observed in the buildings was the discontinuity of frames in the plan. Continuous and regular frame lines that provide uniform distribution of forces and proper transfer of earthquake load do not exist. The beam and columns were simply oriented and arranged according to the architectural plan. So, the beams are generally discontinuous and supported by girders. Thus, discontinuous and zigzagged beam lines were observed, resulting in poor seismic performance.



Fig 6.12 Localized heavy damage

The following remarks summarize our field observations in Bayraklı after the İzmir Seferihisar offshore (Samos) earthquake:

- 1- The ground motion accelerations measured in the center of İzmir after Seferihisar earthquake are generally very low, reaching high values in Bayraklı due to its special site conditions. However, the relatively high spectral accelerations recorded at mid-to-long period range due to soil amplification are below the design basis values.
- 2- The İzmir Seferihisar offshore (Samos) earthquake resulting in site amplification, especially in the period range of 0.8-1.4 seconds, caused heavy damage on inadequately designed and/or constructed 7-10 story reinforced concrete buildings in Bayraklı. Thus, in the design of multi-story buildings in Bayraklı and similar regions, soil amplification should be taken into account, and the use of site-specific response spectrum should be considered.

- 3- Infill wall damage observed in many buildings resulted in significant property loss and played an essential role in the earthquake aftermath psychology of people. Even if no structural damage was observed in the buildings, it caused the buildings to be perceived as excessively damaged.
- 4- It was observed that the buildings that appear to have no damage from a street survey might have experienced significant damage when examined from inside.
- 5- As evidenced in the case of Barış apartment complex, infill walls have a beneficial contribution to the vertical and lateral load-carrying capacity of buildings, reducing the drift demand and thus preventing the collapse of buildings under small and medium size earthquakes.
- 6- Inadequate stiffness and strength of slabs and tie-beams, transferring the load to shear walls led to high drift demands in the building resulting in a concentration of damage in nonstructural members.
- 7- In most damaged buildings, a regular structural system and continuous frame system, required for a proper earthquake load transfer, was not established in the examined buildings.
- 8- Excessive level of corrosion was observed in bottom ends of columns located at the basement and ground floors of examined buildings in Bayraklı, İzmir.
- 9- Local overhang-column connection and ground floor column damages observed at the cantilevers of 7-10 story buildings are so high that the retrofit and re-occupation of the buildings was impossible.
- 10- The damages observed are due to inadequacies and deficiencies present in the buildings; the fact that the levels of ground motions measured are less than the design levels is a clear indication of this phenomena. Therefore, this earthquake should not be considered as the design level earthquake. Consequently, the impression that the buildings suffering no damage have adequate seismic capacity would be quite misleading.

6.3 Tall Buildings

The tallest building in İzmir, the 216 m tall 48-story Mistral İzmir Office Tower in Konak district, has been monitored since January 27, 2019 within the scope of a research project entitled “Guidelines for Structural Health Monitoring Systems on Tall Buildings and a Case Study,” which is undertaken at METU and funded by the Disaster and Emergency Management Presidency of Turkey (AFAD) under its National Earthquake Research Program. The building was permanently instrumented with a 27-channel structural health monitoring system (Fig 6.13) and vibration records from the building and seven AFAD strong motion stations in the vicinity of the building have been streamed in real time to METU (Gumus and Celik, 2019). Recorded floor accelerations and calculated floor displacements during the M_w 6.6 İzmir Seferihisar (Samos) earthquake (30.10.2020 14:51:24) are presented in Fig 6.14. The maximum floor acceleration is 0.28 g at the 48th floor and 0.11 g at the second basement while the maximum displacement is 16 cm at the 48th floor. No damage was reported, and the building is in continued use following the earthquake.

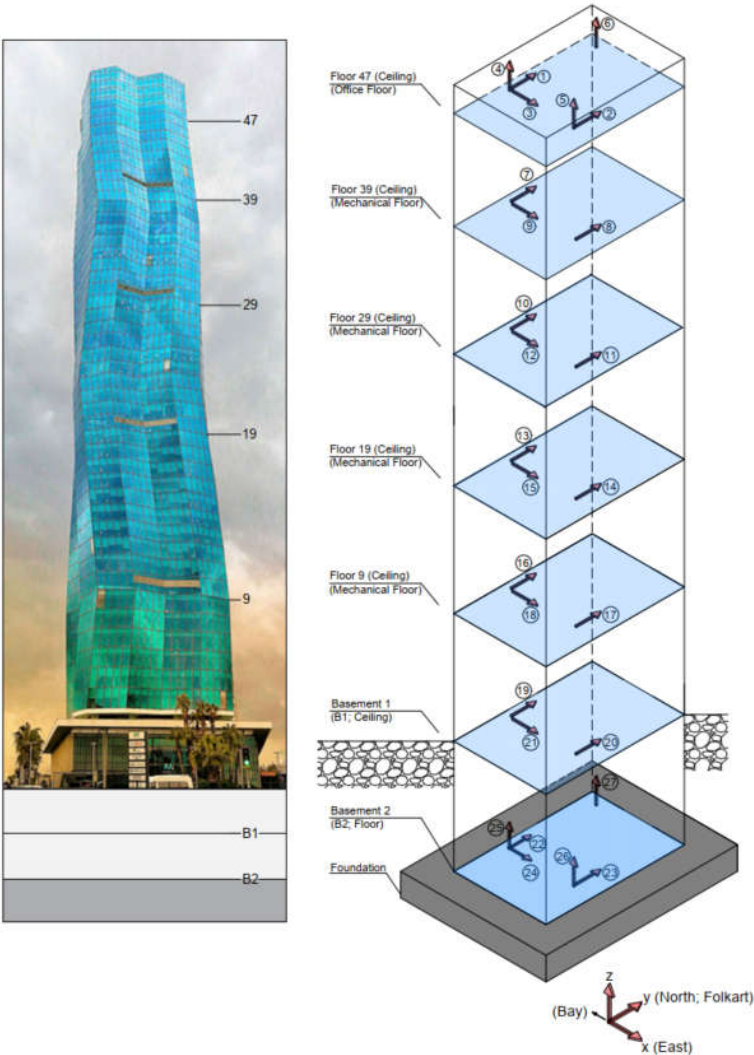
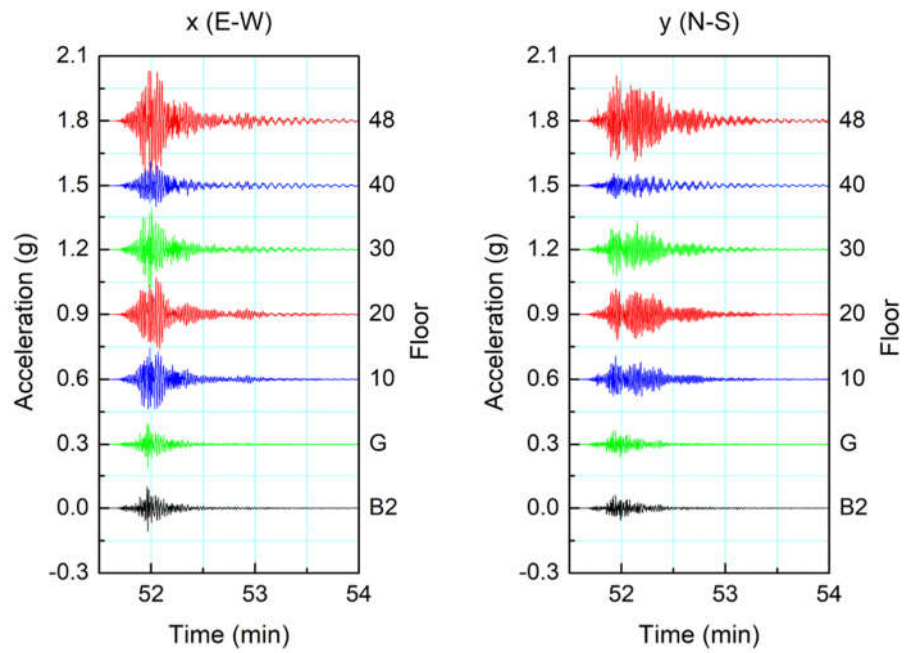


Fig 6.13 Instrumentation scheme



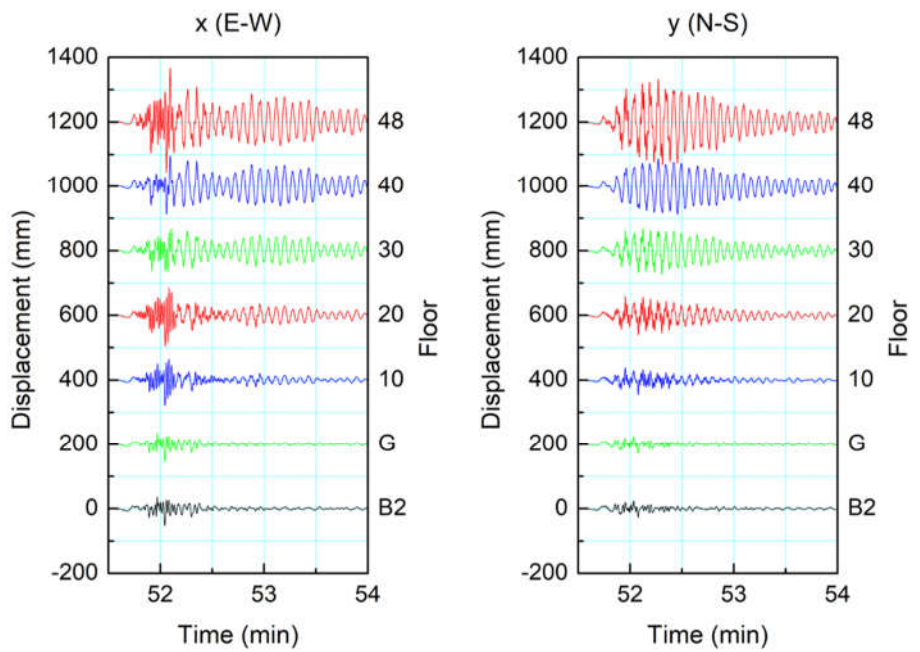
Floor Accelerations



Max acceleration: 0.28 g (48th floor), 0.11 g (2nd basement)



Floor Displacements



Max displacement: 16 cm (48th floor)

Fig 6.14 Floor accelerations and displacements

6.4 Bridges

The bridges on Mürselpaşa Caddesi - Zafer Payzın highway line were examined in detail after the Mw 6.6 magnitude İzmir Seferihisar (Samos) Earthquake that took place on October 30, 2020. The visited line is highlighted in yellow below (Fig 6.15).

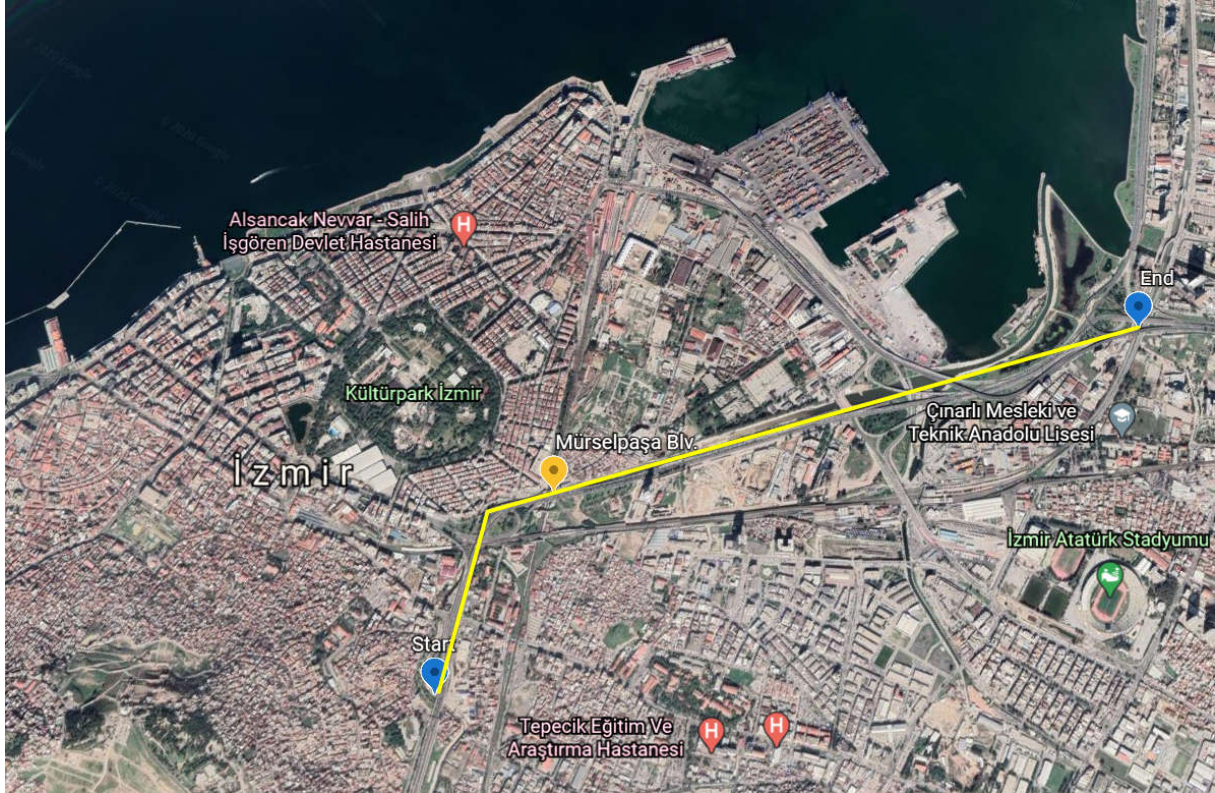


Fig 6.15 Inspected line

As is known, the bridges are approximately 70 km from the earthquake epicenter. No permanent movement has been observed in the superstructure beams and supports. The bending or shear capacity of the bridge columns and foundations has not been exceeded and no cracks have occurred due to the recent earthquake. There was no settlement on the foundation over soft soil. No movement was observed at the bridge expansion joints. No loss of function such as rupture or fracture has been observed in non-structural bridge elements (precast panels, pedestrian railings, lighting poles, etc.). The earthquake performances of longitudinal joints between twin bridges are adequate as expected and some small concrete pieces not more than 2-3 cm fall on the ground only at some very local zones. After the examination of the superstructure and infrastructure of the bridges, no earthquake-related damage was detected.

The structural history of the bridges could not be documented after the transfer of ownership from KGM to the municipality. Mürselpaşa Street-Zafer Payzın bridge highway line rehabilitation project has been started before the earthquake in September 2019 and includes the maintenance, repair and identification of seismic performance of the bridges, Highway,

Connection Roads and Large Art Structures Application And Improvement and strengthening studies continue within the scope of the Strengthening Projects. Most of the cracks observed since the beginning of the project caused by rainwater and are ASR (Alkali-Silica Reaction) cracks, which are the result of a chemical reaction that occurred years ago in the bridge elements. These chemical cracks did not grow after the earthquake. The repair of these cracks will be carried out within the scope of the related project (Fig 6.16 and Fig 6.17).



Fig 6.16 ASR based cracks (non-seismic) and general view

Bridges were immediately available for use just after the earthquake. As a result, it was determined that bridges that performed successfully during the earthquake were usable without the need for emergency intervention.



Fig 6.17 Typical before and after earthquake photo (December, 2019) & (November 2020)

Bridge girders, which were started to be built 20 years ago and stopped after a while fell during the earthquake because their lateral stability has not been provided for the last 20 years. These bridges were not on the highway line under investigation (Fig 6.18).



Fig 6.18 Stopped construction of bridges 20 years ago without lateral girder stability (10 years ago and now)

Consequently, the bridges which are checked at every stage of the design, construction and are subject to building inspection, have proved to be successful in terms of earthquake performance and provided the condition of immediate use, as in the Van 2011 and the Sivrice 2020 earthquakes.

References

AFAD Deprem Dairesi Başkanlığı (2020), 30 Ekim 2020 Ege Denizi, Seferihisar (İzmir) Açıkları (17.26 km) Mw 6.6 Depremine İlişkin Ön Değerlendirme Raporu, AFAD.

Akka, S., Sandıkkaya, M. A., Bommer, J. J. (2014). Empirical ground-motion models for point-and extended-source crustal earthquake scenarios in Europe and the Middle East. *Bulletin of earthquake engineering*, 12(1), 359-387, <https://doi.org/10.1007/s10518-013-9461-4>.

Bilal, M. and Askan, A. (2014), Relationships between felt intensity and recorded ground motion parameters for Turkey, *Bull Seism. Soc. Amer.*, 104, 484–496, <https://doi.org/10.1785/0120130093>.

Demirtaş, R. (2019), İzmir İli, Menderes İlçesi, Değirmendere, Gümüldür ve Özdere Mahallelerinin Paleosismolojik Ve YüzeY Faylanması Tehlike Zonu Açısından Değerlendirilmesi 10.13140/RG.2.2.14234.70087.

GMT 5: Wessel, P., W. H. F. Smith, R. Scharroo, J. Luis, and F. Wobbe, *Generic Mapping Tools: Improved Version Released*, *EOS Trans. AGU*, 94(45), p. 409–410, 2013. <https://doi.org/10.1002/2013EO450001>.

Gumus O and Celik O.C. (2019) Structural Health Monitoring System on a 216 m Tall Building in Izmir per the New Turkish Building Earthquake Code, *Proceedings of the Fifth International Conference on Earthquake Engineering and Seismology*, October 8–11, Ankara, Turkey.

Pamuk, E., Gönenç, T., Özdağ, Ö. C., & Akgün, M. (2018). 3D Bedrock Structure of Bornova Plain and Its Surroundings (Izmir/Western Turkey). *Pure and Applied Geophysics*, 175(1), 325-340.

TBEC, Turkish Building Earthquake Code (2019). Ministry of Interior, Disaster and Emergency Management Presidency (AFAD).

TEC, Earthquake Code of Turkey (2007). Specification for Buildings to be Built in Seismic Zones, Ministry of Public Works and Settlement, Government of the Republic of Turkey.

TEC, Earthquake Code of Turkey (1975). Specification for Buildings to be Built in Disaster Zones, Ministry of Public Works and Settlement, Government of the Republic of Turkey.

USGS Liquefaction Susceptibility Map (last visited November 9 2020) <https://earthquake.usgs.gov/earthquakes/eventpage/us7000c7y0/executive>